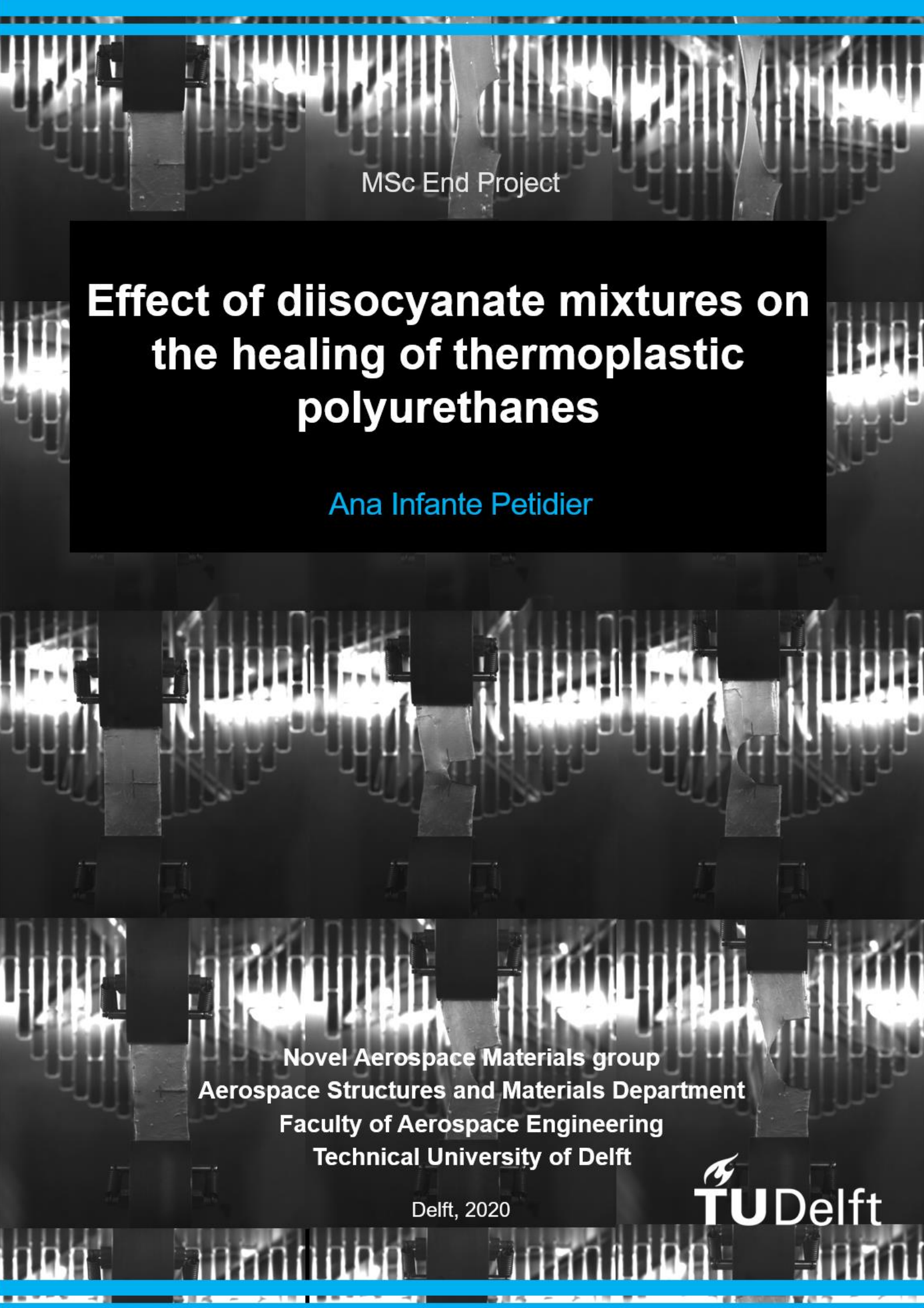

MSc End Project

Effect of diisocyanate mixtures on the healing of thermoplastic polyurethanes

Ana Infante Petidier

Novel Aerospace Materials group
Aerospace Structures and Materials Department
Faculty of Aerospace Engineering
Technical University of Delft

Delft, 2020

TU Delft

Master of Science End Project

For the completion of the MSc in Industrial Engineering by the University of Sevilla
(Trabajo Fin de Máster – 51460032 – 12 ECTS)

Effect of diisocyanate mixtures on the healing of thermoplastic polyurethanes

Author:
Ana Infante Petidier

Supervisor:
Dr. S. J. García

Novel Aerospace Materials group
Aerospace Structures and Materials Department
Faculty of Aerospace Engineering
Technical University of Delft
Delft, 2020

Novel Aerospace Materials group
Aerospace Structures and Materials Department
Faculty of Aerospace Engineering
Technical University of Delft

Author: Ana Infante Petidier
Supervisor: Dr. Santiago J. García Espallargas

GRADUATION COMMITTEE

Chair holder:

_____
Prof. Dr. Ir. Sybrand van der Zwaag

Committee members:

_____
Dr. Santiago J. García Espallargas

_____
PhD candidate Vincenzo Montano

Delft, July 2020

To my family

To my friends

From creating molecules to building aircrafts.

-NovAM-

Acknowledgement

This project is the result of the research conducted at Novel Aerospace Materials (NovAM) group at the Delft University of Technology. It constitutes the end of two years of study for the completion of the MSc in Industrial Engineering at the University of Sevilla. This project would not have been possible without the contribution of many people.

I would like to thank my supervisor, Santiago J. García Espallargas, for allowing me to become part of this research group, for being an endless source of ideas and for guiding me during the last eight months. I would also like to thank Vincenzo Montano, for always sharing his broad knowledge about polyurethanes, for always being willing to give a hand with the experimental part and for his good advice. I would also like to express my admiration and gratitude to Sybrand van der Zwaag, for his practical ideas and critical mindset and for always having a response for all issues. Special thanks go to Linda Ritzen, a perseverance role model from whom I learnt the basics of this project.

A vital part of this research is all NovAM members, who have all contributed in some way to this project. Especially, I would like to thank Bert van der Spek, for the enriching discussions and his help in the most practical part of Chemistry. I would also like to express my appreciation to Shanta Visser, for keeping this great group running.

I would also like to express my gratitude to the personnel of Delft Aerospace Materials and Structures Laboratory, in particular to Marlies Nijemeisland, for her patient and her assistance with the tests performed and to Johan Bijleveld, for sharing his extensive expertise of polymers. I would especially like to thank Gertjan Mulder for his help combined with his professionalism and the nice talks.

I would like to express my gratitude to the European Union for the Erasmus program, which gave me the opportunity to complete the second year of my master at TU Delft and to conduct my final project at NovAM group.

I would like to thank all my friends, who helped me to become the person I am. To my friends from Spain and the new friends, from the Netherlands and from all over the world, met in Delft, I have learnt from them professionally and personally in innumerable aspects. Special thanks go to Mari Ángeles Galvarro Cano and Ventsislav Pazhev, for their great support under all circumstances this year.

Finally, any of this would have been possible without the unconditional support of my family. Thanks for showing me the importance of effort and perseverance and for supporting me in every decision.

Ana Infante Petidier

Delft, 2020

Abstract

Self-healing materials and, in particular, polymers are characterized by their ability to partially or fully restore their original properties or functions after damage. Amongst the healable polymer classes, thermoplastic polyurethanes have received increasing attention in the last years. This is mainly due to their broad application areas, the variety of chemical platforms that can be used, and the potential use of hydrogen bonding to assist the healing process. However, the combination of good mechanical properties and healing at near room temperature remains challenging. In order to learn how to find a better balance between healing and mechanical properties, dedicated studies on the impact of the monomer chemical architecture on the overall polymer performance are needed.

In this work we study the impact of monomer mixtures with different chemical composition on the overall mechanical and healing behaviour of self-healing thermoplastic polyurethanes based on CroHeal™ 2000, biopolyol. The polymers are synthesized via one-shot technique, starting from three constituents: a long chain diol (CroHeal™ 2000), a chain extender (EHD) and a diisocyanate (aromatics - MDI and PPDI, and aliphatic - HMDI) or diisocyanate mixtures (MDI/HMDI and MDI/PPDI in different ratios).

Fracture tests using Single Edge Notch Tension specimens show a clear increase in mechanical properties and interfacial strength recovery after damage for short healing times at room temperature when using higher aromatic content in the isocyanate mixture. Furthermore, IR mapping showed that initial compositional heterogeneity is decreased when more aliphatic isocyanates are used but also when longer annealing times are applied in the case of aromatic diisocyanates. The presence of compositional heterogeneities does not influence the healing response under the conditions studied.

Keywords: self-healing, polymers, TPU, polyurethane, aliphatic diisocyanate, aromatic diisocyanate.

Index

INDEX OF TABLES

INDEX OF FIGURES

Notation

ATR	Attenuated Total Reflectance
DBDI	4,4'-Dibenzyl Diisocyanate
DSC	Differential Scanning Calorimetry
EHD	2-Ethyl-1,3-Hexanediol
FTIR	Fourier-Transform Infrared Spectroscopy
G'	Shear storage/elastic modulus
G''	Shear loss/viscous modulus
H	Hydrogen
HE	Healing Efficiency
HMDI	4,4′-Methylenebis(Cyclohexyl Isocyanate)
HS	Hard Segments
IR	Infrarred Spectroscopy
MDI	4,4′-Methylenebis(Phenyl Isocyanate)
PPDI	1,4-Phenylene Diisocyanate
PU	Polyurethane
RT	Room temperature
SS	Soft Segments
tan(δ)	Ratio of energy lost per energy stored (G''/G')
T_d	Thermal degradation temperature
T_{end}	Endothermic peak temperature
T_g	Glass transition temperature
TGA	Thermogravimetric Analysis
T_m	Melting temperature
TPU	Thermoplastic Polyurethane
wt.	Weight
η	Viscosity

1 INTRODUCTION

As long as you're learning you're not old.

- Rosalyn Sussman Yalow-

Self-healing materials are capable of mimicking the behaviour of biological materials, being able to partially or fully recover their functionality after damage. This novel type of materials entails a progress from the classical *damage management* approach to a *damage prevention* concept [1] and provides clear advantages for applications where high reliability is required and accessibly to repair is difficult or not possible [2].

The self-healing concept started in the 1960s when self-healing properties were first observed in a polymeric material [3]. Nowadays, the self-healing behaviour has also been extended to metals, ceramics and concrete. All these classes of self-healing materials have one common requisite: local temporary mobility [4]. The recovery of the initial properties of the material can be achieved from the microscale to the macroscale depending on the type of material and healing mechanism [2].

Two different healing approaches can be distinguished in these materials. Intrinsic self-healing materials have the capability of inherently healing due to the presence of reversible chemical bonds. Extrinsic self-healing materials recover thanks to the addition of discrete particles containing external healing agents [2][5]. Intrinsic self-healing materials have the advantage that they can heal several times in the same area in contrast to intrinsic self-healing materials that can only heal once as they depend on a healing agent [5]. Structure, chain mobility and density of reversible bonds are crucial for intrinsic self-healing materials [5][6]. Examples of intrinsic self-healing systems that show healing behaviour at room temperature are based on hydrogen bonds and aromatic interactions [5].

This work addresses the study of intrinsic self-healing polymers and, in particular, thermoplastic polyurethanes. To outline the significance of this research and provide basic theoretical background to the reader, the following pages briefly discuss the state of the art on this topic.

1.1 Introduction to intrinsic self-healing polymers and thermoplastic polyurethanes

Between the different healing approaches and classes of materials, intrinsic self-healing polymers stand out due to their ease of mobility at low temperatures [2]. When a polymer network is subjected to mechanical damage; chain cleavage and/or slippage occurs, leading to the formation of reactive groups. In self-healing polymers, the reactivity of these groups is high and, therefore, these groups reassemble and repair the damaged area [7].

The dynamic bonds found in intrinsic self-healing polymers can be mainly classified as covalent chemistry and supramolecular chemistry. Dynamic covalent bonds are a very powerful approach to develop self-healing

polymers. They can be found in Diels-Alder reaction, urea bonds, siloxane bonds, disulphide bonds, acylhidrazone bonds, ester bonds, hemiaminal linkages, alkoxyamine linkages and diarylbibenzofuranone linkages [8]. Supramolecular chemistry refers to the formation of non-covalent secondary interactions between molecules [9]. Some examples of supramolecular chemistry used in self-healing polymers are H-bonding, metal-ligand coordination and π-π stacking [7]. Supramolecular interactions are specially interesting in comparison to covalent bond interactions due to the reformation of the bonds at mild temperatures [10].

In particular, hydrogen bonds exhibit many beneficial properties. Although these bonds are weaker than other supramolecular interactions, their directionality and affinity make possible to achieve high mechanical properties. Moreover, it has been widely demonstrated that the combination of multiple H bonds into a unit of urea isopyrimidone (Upy) leads to an enhanced strength in the association between Upy and polyesters, polyethers and polysiloxane [7]. The concentration and the strength of H bonds highly influence the mechanical strength and the healing response [10].

Apart from hydrogen bonds, studies of heterogeneous networks consisting of soft and hard segments demonstrate their ability to rearrange upon mechanical damage. The local variations of T_g of these networks facilitate the spontaneous rearrangement of the network, exhibited by increased entropy and re-bonding. While the healing of dynamic bonds occurs at Angstrom (Å) levels; star, block and branched polymers show the phase segregation at μm to mm scale [10].

Both H bonds and heterogeneous networks are found in a well-known type of polymers: polyurethanes (PUs). A broad variety of structures are considered to be PUs, with the main common characteristic of the presence of a urethane group (-NHCO-O-) on the macromolecular chain. This urethane group is normally formed by the reaction between the alcohol and the isocyanate groups (Figure 1.1) [11].

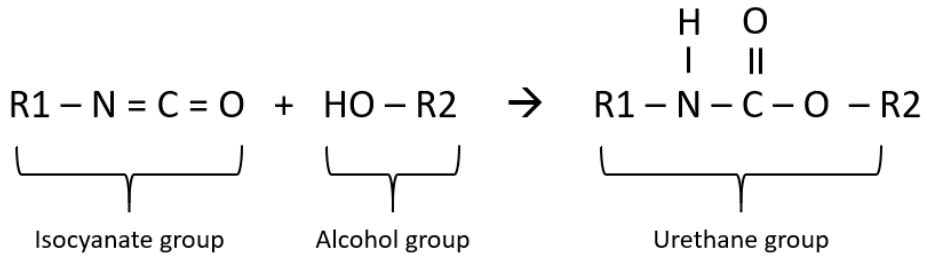

Figure 1.1: Chemical reaction between an isocyanate group and an alcohol group to form an urethane group.

PUs are typically synthesized by reacting these constituents: a long chain diol or macrodiol, a small chain extender diol and a diisocyanate [11]. This synthesis leads to the formation of (AB)n copolymers, consisting of soft segments (SS) and hard segments (HS) (Figure 1.2 (a)). The SS are normally flexible and non-polar and formed by the long chain diol (a polyether or a polyester macroglycol) [12][13]. The HS are rigid and highly polar and formed by the diisocyanate and the chain extender [12]. The glass transition of the SS tends to be below room temperature while the glass transition of the HS is frequently above room temperature. The urethane groups are mainly located in the hard blocks and they tend to form intermolecular H bonds [11].

The HS are grouped into hard domains [11] that act as physical crosslinks and are responsible for the elastomeric behavior of the material [13], as displayed in Figure 1.2 (b). The soft phase or soft domains are the result of the concentration of the long polymeric chains that form the SS. In the micrometre scale, areas with a higher concentration of hard domains, referred as microdomains or disperse phases, and areas with a dominance of soft phases, referred as matrix, are evidence of the characteristic heterogeneous network of PUs (Figure 1.2 (c)). This phenomenon of phase segregation at the micrometer scale has previously been studied with techniques such as Atomic Force Microscopy (AFM) [14] and FTIR mapping [15]. FTIR mapping has the advantage that not only information regarding the shape and area percentage of these microdomains is obtained but also compositional information. The relation between healing and the appearance of these disperse phases shows promise for further studies.

PUs can be either thermoplastic or thermoset. The behavior of thermoplastic polyurethanes (TPU) ranges from a typical soft thermoplastic elastomer to a rigid thermoplastic depending on their chemistry. They are used in a wide range of applications such as biomaterials, coatings, membranes, textile fibers and adhesives [16]. Furthermore, their flexible polymer network characteristics and presence of H bonds makes them good candidates to develop self-healing polymers [5].

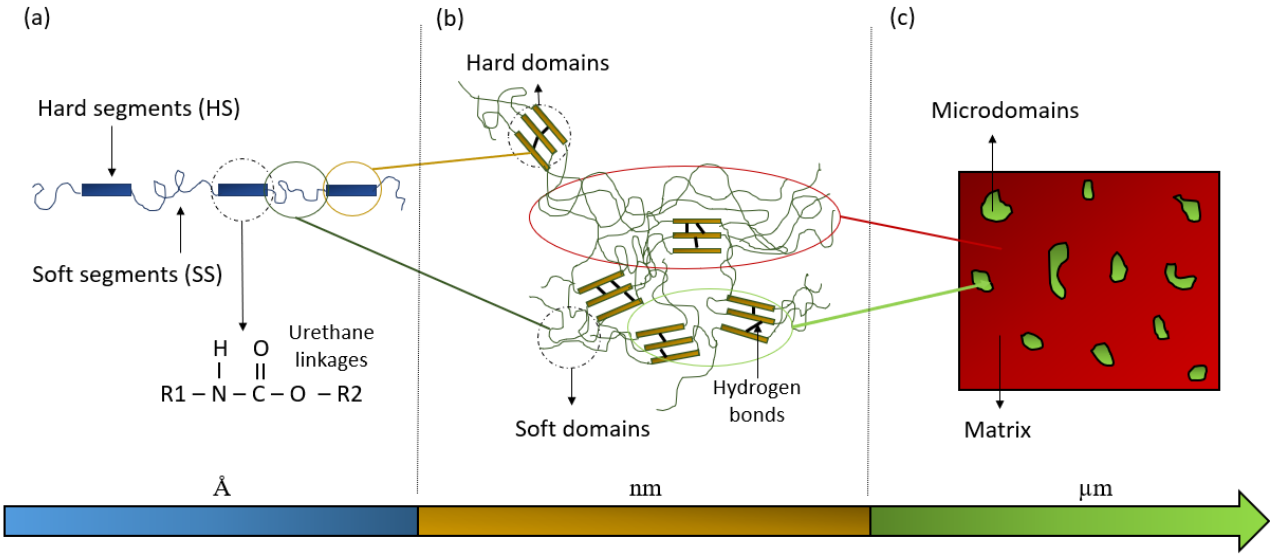

Figure 1.2: Scheme of the phase structure of segmented polyurethanes: (a) block copolymer divided into HS and SS, (b) HS are grouped into hard domains and SS into soft domains and (c) disperse phases or microdomains detected in the µm scale referring to larger presence of hard domains.

The performance of TPUs is typically influenced by their phase morphologies, consisting of hard domains dispersed in a soft segment matrix. It is normally accepted that the driving force generating this phase segregation is the strong hydrogen bonding that exists in the urethane hard segments [16]. Nevertheless, other factors also influence the phase segregation of TPUs [11][16]:

- Chemical structure of soft segments, isocyanates and chain extender.
- Molecular weight of the soft segments.
- Symmetry of the isocyanate.
- Length distribution of the hard segments.
- Ratio between hard segments and soft segments.
- Crystallization of soft and hard segments.
- Solubility between hard and soft segments.
- Polymerization procedure: one step or two steps (prepolymer method).
- Interfacial region between hard segments domains and soft segment matrix.

The polymerization procedure used to prepare polyurethanes can be classified according to the medium (water, bulk, solution) or the order of addition of reactants (one step or two steps method). In the one step or one-shot polyaddition method, all the reactants are added at once. The main consequence is irregular block sequences and higher crystallinity due to the promoted reaction between the glycol and the isocyanate. Nevertheless, the process is fast, reproducible and easy. In the two steps or prepolymer method, first the SS reacts with an excess of diisocyanate and then the chain extender is added. The copolymers obtained through this second method tend to have a more regular structure and better mechanical properties [11].

In [17] and [18] polyurethane elastomers based on mixtures of diisocyanates (4,4′-Methylenebis(Phenyl Isocyanate) (MDI) and 4,4’-Dibenzyl Diisocyanate (DBDI)) were synthesized via different procedures. One procedure consisted of copolyurethane elastomers from two isocyanates that were randomly distributed. For this, a mixture of MDI and DBDI was added to the polyol. Another procedure contemplated copolyurethane elastomers from two isocyanates with selective distribution. In this second option, the polyaddition was performed in two steps. Firstly, MDI was added to the macrodiol, obtaining a prepolymer and then DBDI was dissolved into the prepolymer. The same procedure was also followed adding first DBDI. Different properties regarding thermal transitions, mechanical resistance and morphology were obtained for the polyurethanes synthesized. For polymers following the first procedure, higher tensile strengths and, in general, better mechanical response were obtained. Moreover, smoother fracture surface was detected for these polymers. This exhibits the impact of the synthesis procedure. Apart from the information already introduced, the data available in literature regarding TPUs with mixtures of diisocyanates is limited, what makes it a potential area of research.

As well as the synthesis procedure, the type of isocyanate and its symmetry has a strong impact on the phase

segregation and the mechanical properties of the polyurethane [11][19]. An increased symmetry may lead to the crystallization of the HS and to better mechanical properties [11]. Two groups of isocyanates are generally distinguished: aliphatic and aromatic [20]. Aliphatic diisocyanates have the advantage of providing color-stable weathering resistance polyurethanes while aromatic diisocyanates tend to undergo discoloration when exposed to UV light [11][20]. However, polyurethane elastomers based on aliphatic diisocyanates are subjected to photooxidation processes degrading the material easier than polyurethane elastomers based on aromatic diisocyanates [20]. The ease of photooxidation increases with the content of hard segments. Aliphatic diisocyanates are costly in comparison to aromatic diisocyanates due to the expensive diamines used to manufacture them [20]. Aromatic isocyanates typically provide high tensile strength and modulus as well as increased thermal stability [11].

Some of the most used isocyanates are 4,4′-Methylenebis(Phenyl Isocyanate) (MDI), 4,4′-Methylenebis(Cyclohexyl Isocyanate) (HMDI) and 1,4-Phenylene Diisocyanate (PPDI). Hydrogenated MDI or HMDI can be listed amongst the preferred aliphatic diisocyanates for polyurethane elastomers. Higher quantities of HMDI increases tensile strength, split tear strength, hardness, resilience and elongation [20]. MDI is one of the most used aromatic isocyanates. This monomer is normally used to manufacture segmented polyurethanes elastomers in the automotive industry. It has a melting point of 41 ºC [20]. PPDI is categorized as a highly symmetrical aromatic diisocyanate. This leads to have a high tendency to undergo dimerization even in solid state and, therefore, it is normally used only for prepolymers. The melting point of PPDI is around 94-96 ºC. As PPDI is around twice more reactive than MDI, catalysts are not generally used. PPDI based polyurethanes present high mechanical properties at elevated temperatures due to its increased crystallinity [20].

1.2 Research objectives and scope

As seen above, TPUs show great promise as self-healing polymers due to their presence of H bonds and, therefore, their ability to heal at mild temperatures. Furthermore, despite the existing body of knowledge on the topic, it can be observed that additional research is needed on the effect of mixtures of diisocyanates. In this respect, the current work addresses the effect of mixture of aliphatic and/or aromatic isocyanates (MDI, HMDI and PPDI) according to different molar ratios on the healing properties of a TPU. Additionally, this project aims at elucidating the impact of the micro-phase segregation on healing.

To achieve this, the synthesis of nine different TPUs was performed: three of them based on one diisocyanate (designated as MDI-p, HMDI-p and PPDI-p) and the rest based on mixtures of diisocyanates (designated as M80/H20, M60/H40, M40/H60, M80/P20, M60/P40 and M40/P60). The TPUs based on mixtures of diisocyanates were characterized via FTIR, TGA, DSC, FTIR mapping, rheology and fracture tests. For the TPUs based on one diisocyanate, the same characterization was conducted except for TGA and DSC due to the extensive research on this topic already performed at NovAM group. Additionally, to elaborate on the observations from these tests, natural ageing and induced ageing of a subset of these TPUs was conducted.

1.3 Outline

This report is divided into six chapters. Chapter 2 covers materials and methods, while chapters 3, 4 and 5 focus on answering the research objectives just stated. Chapter 3 provides an overview of the TPUs based on one isocyanate and introduces the relevance of mixture of isocyanates. Chapter 4 addresses the main research question: effect of combination of isocyanates on the self-healing properties of TPUs. Chapter 5 aims at clarifying previous results included in chapter 3 and 4 via the concept of ageing. Finally, in chapter 6 the conclusions and recommendations based on this research are presented.

2 MATERIALS AND METHODS

I'm truly glad I've managed to get the public interested in questions about basic research.

- Ada Yonath-

In this chapter a generic overview of the materials used in the project as well as the characterization methods covered is provided. Any specific change required for a particular polymer will be specified in the following chapters.

2.1 Materials

The materials utilized for the synthesis of the polymers were: CroHeal™ 2000, a biobased polyol provided by Croda Nederland B.V.; 2-Ethyl-1,3-hexanediol (EHD; 97%, mixture of isomers), a short chain diol purchased from Sigma-Aldrich and used as chain extender; and three different types of diisocyanates: 4,4′-Methylenebis(phenyl isocyanate) (MDI; > 97%), 4,4′-Methylenebis(cyclohexyl isocyanate) diisocyanate (HMDI; > 90%, mixture of isomers) and 1,4-Phenylene diisocyanate (PPDI; > 98%), all purchased from TCI Europe N.V. The chemical structures of the different polyurethane components are shown in Figure 2.1. The complete structure of CroHeal™ 2000 is not shown for confidentiality reasons.

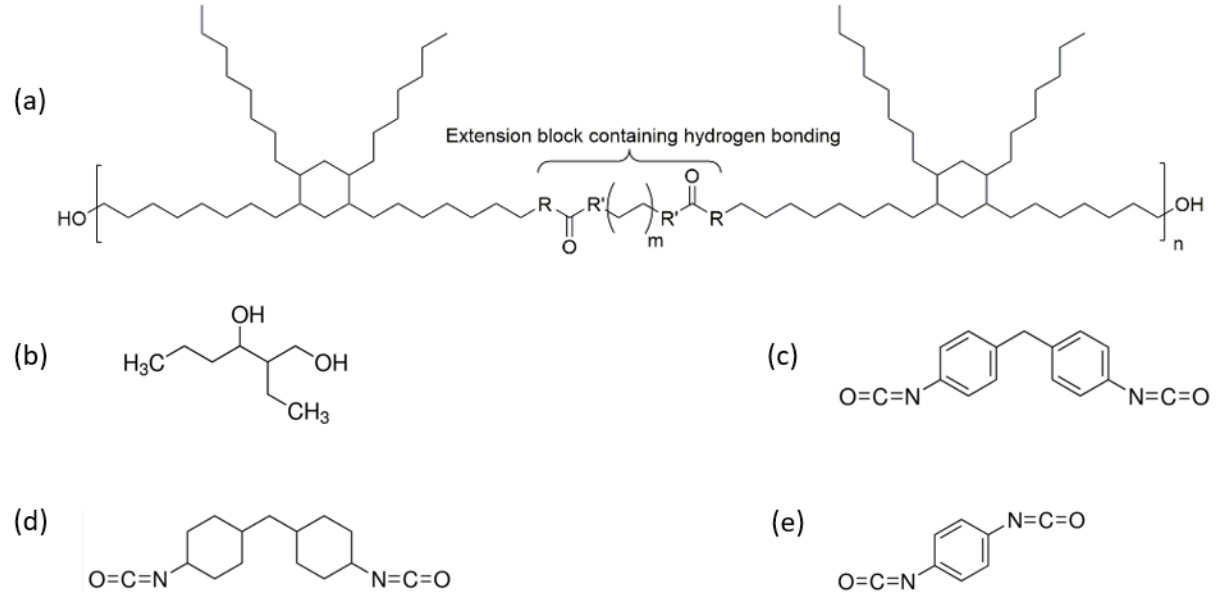

Figure 2.1: Molecular structure of: (a) CroHeal™ 2000, (b) EHD, (c) MDI, (d) HMDI and (e) PPDI.

2.2 Methods

Different characterization methods were used in order to assess the features of each polymer, emphasizing the importance of the correlation microstructure and healing properties.

Fourier Transform Infrared Spectroscopy (FTIR)

Attenuated Total Reflection Fourier Transform Infrared (ATR-FTIR) spectroscopy in the range 4000 cm^{-1} to 550 cm^{-1} was used to first test all TPUs with a Perkin Elmer Spectrum 100 FTIR Spectrometer performing 16 scans with a resolution of 4 cm^{-1}. This test allowed to study the completion of the reaction and the hydrogen bonds formed.

Thermogravimetric analysis (TGA)

Perkin Elmer TGA 4000 was used to determine the degradation temperature of the polymers. The analysis was set from 30 ºC to 600 ºC at 10 ºC/min under nitrogen environment to prevent oxidation.

Differential Scanning Calorimeter (DSC)

A TA DSC 250 was employed to measure the thermal transitions. The program used consisted of two full loops of heating and cooling under nitrogen. First, the sample was stabilised at 30 ºC, after, it was cooled down to -50 ºC, staying at -50 ºC for 5 min; then, it was heated up until 150 ºC and kept at this temperature for 5 min. After the first heating ramp the sample was cooled down again to -50 ºC. Following the first cooling the sample was exposed to the same heating-cooling profile (-50 ºC – 150 ºC and 150 ºC – -50 ºC). Finally, the sample was heated up and stabilised at 30 ºC. All heating and cooling rates were 5 ºC/min.

FTIR mapping

FTIR mapping (also found in literature as FTIR micro-spectrometry) is an extension of ATR-FTIR spectroscopy where an infrared interferometer combined with a microscope allows to obtain chemical maps of the surface of a sample in the micrometre scale. This high resolution makes it possible to analyse compositional changes in polymer systems [21].

A Perkin Elmer Spotlight 400 FTIR Imaging System was used in the range 4000 cm^{-1} to 690 cm^{-1} in ATR mode, allowing to observe the local composition variations in the TPUs synthesized. The analysed area was 500 µm x 500 µm and the selected pixel size, 1.56 µm, with 2 scans per pixel. With the help of ImageSpectra Software, a principal component analysis was carried out. This analysis provided images where two main components were detected: disperse phases and matrix. The images showed a double colour scale (from black to bright green for disperse phases and from black to bright red for the matrix) according to the different FTIR spectra obtained in the area (Figure 2.2). Bright red showed a composition significantly different from bright green, while black/grey was normally attributed to transition areas between both compositions. The percentage of disperse phases was also provided by the software. At least three measurements per sample were conducted to precisely quantify the percentage of disperse phases.

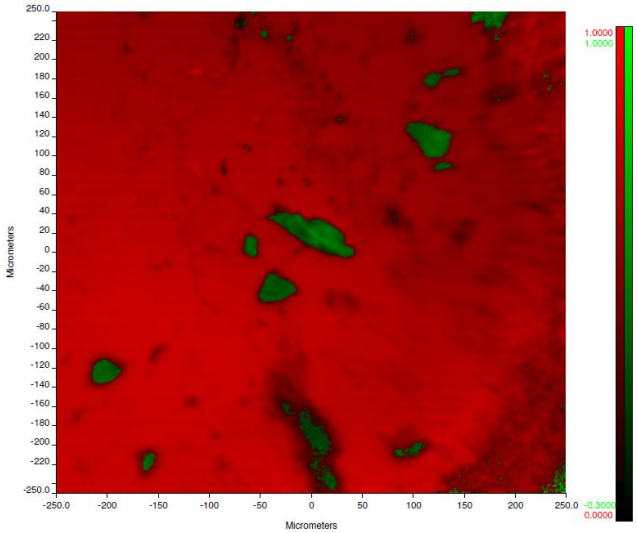

Figure 2.2: Example of FTIR mapping image showing the colour scale.

Rheology

Rheology was used to study the viscoelastic behaviour of the samples. The samples used were cylindrical with 8 mm diameter and between 2.2 mm and 3.2 mm thickness. Two tests were conducted in a Thermo Scientific Haake MARS III Rheometer-FTIR with 8 mm parallel plates:

- Oscillatory shear strain sweep test: from 0.001 % to 10 % shear strain amplitude at 1 Hz. The application of this test was to identify a shear strain amplitude within the Linear Viscoelastic Region (LVR) for the temperature sweep.
- Oscillatory temperature sweep test: from 30 ºC to 250 ºC at 3 ºC/min at 1 Hz. The shear strain amplitude sweep used was 0.1 % for all polymers.

Fracture test

Instron model 3365 universal testing device equipped with 1 kN load cell and with wedge action grips was used to conduct fracture tests. A crosshead speed of 0.5 mm/s and a temperature of 10 ºC were set as testing conditions based on facilitating the observation of the crack opening and propagation and on always being above the glass transition temperature ($T > T_g$).

Single-Edge Notch Tension (SENT) specimens with dimensions of 70 mm x 20 mm (length x width) were employed, as shown in Figure 2.3 (a). The average thickness of the samples varied from 2.50 mm to 3.00 mm. In the samples subjected to longer annealing times, the thickness varied from 2.50 to 3.50 mm. The thickness was averaged considering 6 different points in both sides of the 70 mm length of the sample. The standard deviation of the measures of any sample did not exceed 0.15 mm. A sharp pre-notch until length of 10 mm was made from the middle of the length, perpendicularly to it (Figure 2.3 (b)). When the samples were clamped, there was a distance of 40 mm between the grips. Optical photos were taken during the test at 10 frames per second (10 Hz) with an Optomotive Velociraptor camera. The total number of photos varied from 300 for the most brittle samples to more than 3000 for the more ductile ones.

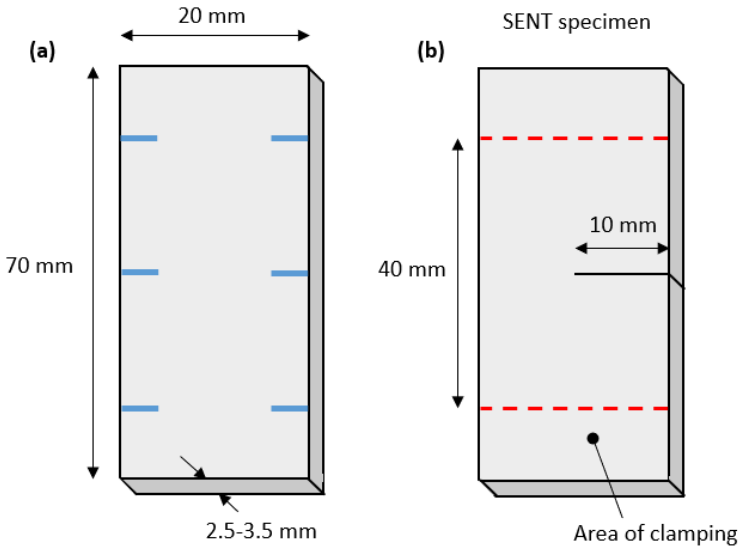

Figure 2.3: Scheme of the fracture test specimens showing: (a) samples obtained after demoulding and die cutting, marking in blue the six measurement points to calculate the thickness and (b) samples with the pre-notch made, outlining the area of clamping.

Healing characterization

Fracture tests were also used to assess the healing efficiency of the samples. According to [5], the fracture procedure provides higher reliability in relation to healing efficiency as other mechanical methods such as tensile tests tend to overestimate the maximum healing efficiency achievable for supramolecular chemistries at RT.

Once the fracture test was conducted, the sample was unclamped and the two parts were brought together until contact by hand for about 10 s. Then, a PTFE film was placed in between the cracked surfaces of the pre-notched area to prevent any healing at this location. After that, the samples were kept inside plastic bags with no external pressure and left at room temperature (22 ± 2 ºC) for one week. To assess the reproducibility of the healing

protocol, two samples were tested per polymer. For M80/H20 and M80/P20, the fracture and healing procedure at the same location was repeated twice to test multiple healing events. The data reported regarding the healing efficiency was calculated as the average value of two samples with the exception of PPDI-p which could only be tested once.

The healing efficiency was calculated as the ratio between the properties measured for the pristine and the healed states according to the equation:

$$Healing\ efficiency\ (HE)_{fracture} = P_{healed}/P_{pristine} \quad (1)$$

where P stands for the mechanical property of interest. The different properties considered were maximum load, maximum displacement and work required to break the sample, as displayed in Figure 2.4.

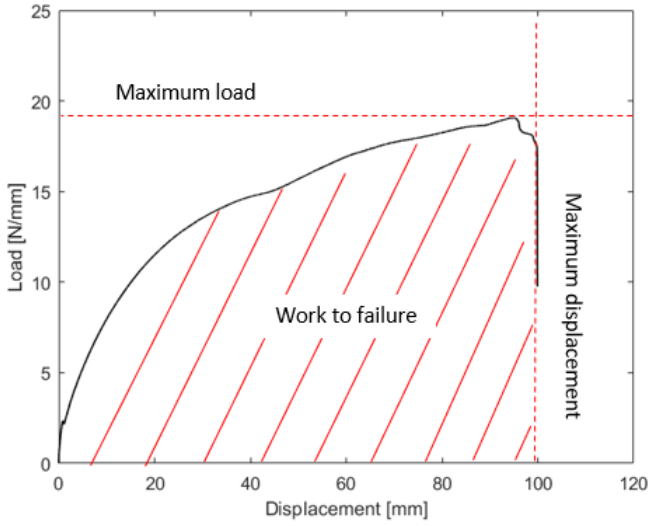

Figure 2.4: Load vs. displacement curve of a fracture test showing the different properties considered to calculated the HE.

3 EFFECT OF THE AROMATIC/ALIPHATIC CHARACTER OF HARD SEGMENTS ON POLYURETHANE COPOLYMERS

Every scientist dreams of doing something that can help the world.

- Tu Youyou-

The main objective of this chapter is to analyse the influence of the diisocyanate selection on mechanical properties and healing of TPUs. MDI-based polyurethanes (MDI-p), HMDI-based polyurethanes (HMDI-p) and PPDI-based polyurethanes (PPDI-p) were synthesized and characterised, specifically focusing on their microstructure and self-healing properties.

3.1 Polymer synthesis

The molar mass and the molar ratios used for the polymerization are displayed in Table 3.1. It should be underlined that the quantity of isocyanate finally used was calculated as a 10 % excess of the mols of CroHeal™ 2000 and EHD. The excess was added to assure full synthesis completion. Moreover, it was demonstrated in [22] that excellent mechanical properties were obtained for the TPUs synthesized when a small excess of diisocyanate in comparison to the polyol mixture was added. The polymer was obtained via one-shot polyaddition synthesis in bulk. The nomenclature for the different polymers refers to the diisocyanate name adding -p to distinguish it from the diisocyanate itself (MDI-p, HMDI-p and PPDI-p).

Table 3.1: Molar mass and molar ratio of the materials used.

	Molar mass [g/mol]	**Molar ratio**
CroHeal™ 2000	2000	1
EHD	146.23	0.6
MDI	250.26	1.7
HMDI	262.35	
PPDI	160.13	

First, CroHeal™ 2000 was placed in an oven at 100 ºC in order to reduce its viscosity and remove the entrapped air. After 25 minutes, approximately 30 g of CroHeal™ 2000 were poured in a propylene cup and put back in the oven at 70 ºC.

For MDI-p, MDI was removed from the freezer (kept at -20 ºC) and left outside for 40 minutes before opening in order to limit the moisture absorbance of the isocyanate. Afterwards, it was weighted in a propylene cup and placed in the oven at 60 ºC. While MDI was being heated, EHD was added to the CroHeal™ 2000 cup with the help of a syringe and placed back in the oven at 70 ºC. After approximately 30 minutes, MDI was removed from the oven and added to the polyol mixture.

For HMDI-p, the liquid state of the isocyanate facilitated the synthesis. In this case, EHD was added to the CroHeal™ 2000 cup and, after that, HMDI was injected.

For PPDI-p, PPDI was removed from the fridge (kept at 2 ºC) and, similarly to MDI, left outside for 40 minutes before opening. Then, PPDI was weighted in a beaker and placed in an oil bath at 120 ºC inside a fume hood. As for the case of MDI, while PPDI was being heated in the oil bath, EHD was added to the CroHeal™ 2000 cup and placed back in the oven at 70 ºC. When PPDI has become fully liquid, it was removed from the oil bath and added to the polyol mixture.

For all cases, the three reactants were mixed using a vacuum assisted high speed mixer (SpeedMixer™ DAC 400.2 VAC-P). In the mixer, the cup was degassed for 20 seconds and then mixed at 2300 rpm. Different mixing times were used, depending on the reaction kinetics of each polyurethane, as reported in Table 3.2. This way, the mixing time increases in the order PPDI-p < MDI-p < HMDI-p according to the higher reactivity of aromatic isocyanates [11] and the higher reactivity of PPDI when compared to MDI [23]. The resultant mixture was poured at room temperature on PTFE moulds with dimensions 70 x 20 x 2.5 mm and placed in an oven for 1 day at 60 ºC to complete the reaction. In order to achieve constant thickness for the fracture samples, these moulds were covered with a PTFE slab and with a stiff aluminium plate with weights on top to achieve a uniform pressure of around 1.6 kPa.

Table 3.2: Steps in the SpeedMixer™ for MDI-p, HMDI-p and PPDI-p.

	1st step - vacuum	**2nd step – mixing – 2300 rpm**
MDI-p	15 s	135 s
HMDI-p		160 s
PPDI-p		105 s

After 24 hours, the moulds were removed from the oven and kept roughly 10 minutes at room temperature. To avoid any deformation of the samples during the demoulding process, plastic bags filled with ice were placed on top of the moulds and when the moulds were cold enough (after approximately 2 hours), they were placed in the freezer at -18 ºC. This way, when the demoulding procedure was executed, the samples were below their T_g and no large plastic deformation took place. As it was difficult to control the quantity of material poured in the mould, some excess could come out when the pressure was applied. This overflow was removed on cut with a shaped die with the target dimensions of 70 x 20 mm.

3.2 Results and discussion

3.2.1 Polymer synthesis

One of the difficulties of the synthesis was attributed to the high viscosity of the CroHeal™ 2000, although when the material was heated enough the handling of the material was considerably improved. Another complication was related to the high stickiness of the polyurethanes, what forced to use low surface tension materials such as PTFE. The procedure previously described in 3.1 Polymer synthesis is the result of several modifications in order to improve the sample quality regarding bubble free and transparent appearance, constant thickness and quantity of unreacted isocyanate.

The weight percentage of hard segments (HS) in the synthesized polymers can be calculated as:

$$\%\, HS_{wt} = \frac{weight\ (chain\ extender) + weight\ (diisocyanate)}{total\ weight\ polymer} \quad (2)$$

Making this calculation, the percentage of hard segments obtained for MDI-p, HMDI-p and PPDI-p is 21 %, 22 % and 16 %. This is less than the typical 30-40 % by weight of hard segments normally found in TPUs [16]. The weight percentage of HS influences the mechanical properties, what should be considered when comparing the three isocyanates. In general, higher tensile strength and less deformation is obtained for larger weight percentages of HS as hard domains can be interpreted as rigid fillers that increase the physical crosslinking content [24].

3.2.2 FTIR

The complete synthesis was confirmed in the MDI-p and PPDI-p. Nevertheless, a small peak at 2250 cm^{-1} was detected in the HMDI-p samples. This peak indicates the presence of free isocyanate (N=C=O) groups, as shown in Figure 3.1 with an arrow. The unreacted isocyanate due to slow reaction could influence the overall mechanical properties and ultimately affect the interpretation of interfacial healing. Different ways to reduce this unreacted isocyanate are included in the appendix. The representative amide I peak, which is widely used to identify polyurethanes due to its relation to C=O and C=N stretching vibration and, therefore, urethane linkages, has been added to the plot. In the case of aromatic isocyanates, this peak appears at higher frequencies than aliphatic isocyanates. This can be associated with a larger ordering of the urethane linkages in aliphatic isocyanates due to their higher mobility.

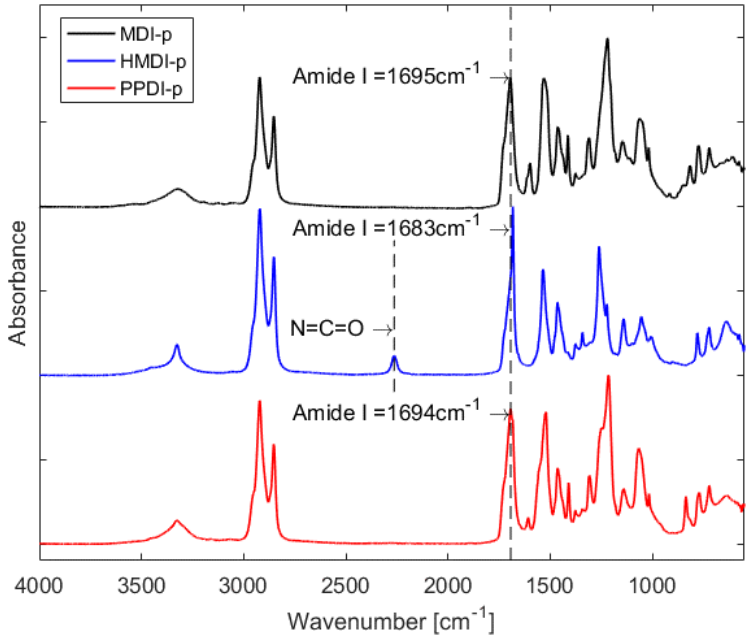

Figure 3.1: FTIR analysis of MDI-p, HMDI-p and PPDI-p.

3.2.3 FTIR mapping

FTIR mapping was used in order to characterise the phase segregation of the material. The characterization of the phase segregation is highly important as it has been demonstrated that it influences the properties of the polymer [16].

Figure 3.2 shows three composition maps obtained with IR mapping. The images show how the quantity of disperse phases with a different composition than the matrix decreases in the order MDI-p, PPDI-p and HMDI-p. These microdomains are characterised by a higher presence of hard domains, as the spectra obtained suggests stronger H bonds in these areas due to the shift of amide I to lower frequencies in the micro-domains when compared to matrix (Figure 3.3).

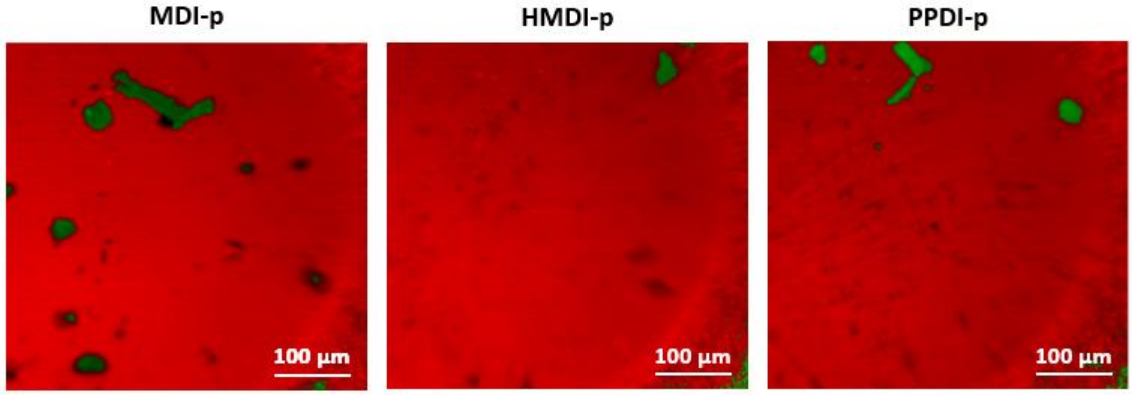

Figure 3.2: ATR-image of MDI-p, HMDI-p and PPDI-p (on the surface of the samples) showing the micro-domains (green) and the matrix (red).

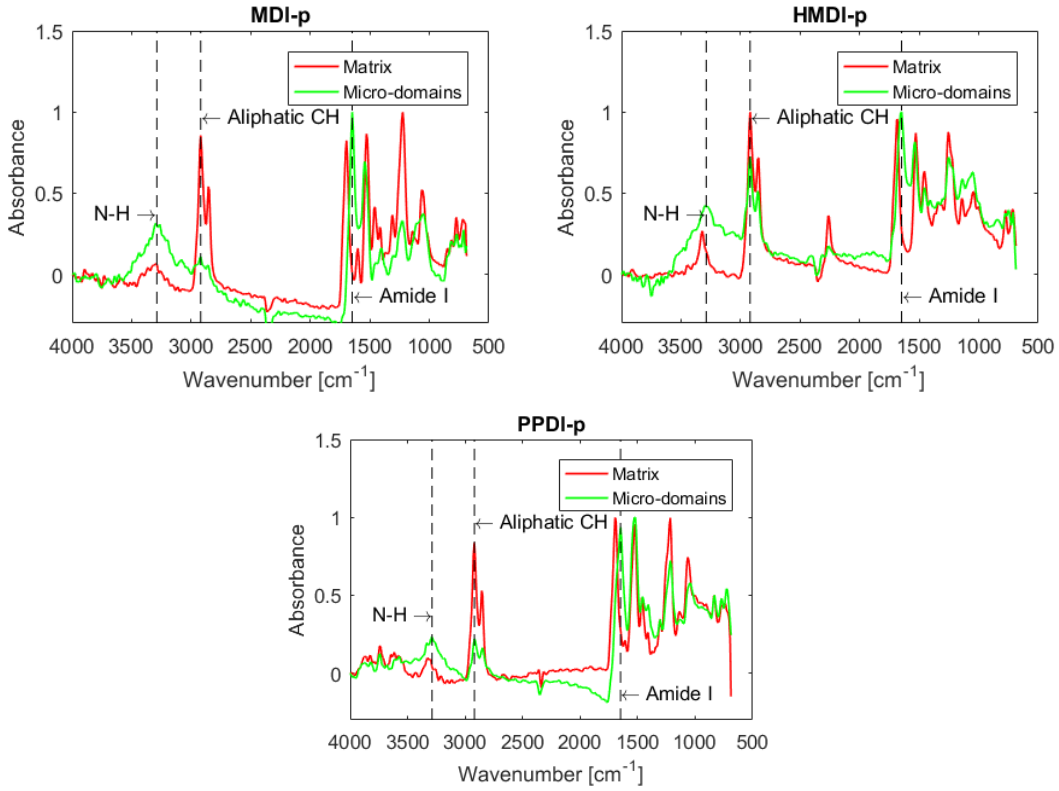

Figure 3.3: FTIR-ATR spectrum of MDI-p, HMDI-p and PPDI-p distinguishing between matrix (red) and micro-domains (green). The relevant peaks are: N-H (3288 cm^{-1}), aliphatic C-H (2290 cm^{-1}) and amide I (1696-1688 cm^{-1} for matrix and 1648 cm^{-1} for micro-domains).

The principal component analysis of ImageSpectra Software used to obtain the images displayed in Figure 3.2 also allowed to conduct a quantitative analysis of the percentage of discretely dispersed phases, as presented in Table 3.3. The values of percentage of microdomains obtained in this project are lower than the values reported in [15] for the same polymers, although the spectra for disperse phases and matrix (Figure 3.3) is the same. One explanation can be the different way to assess the microdomains percentage. Different threshold applied, different software and/or different scale between samples can lead to very different results. For these measurements a scale from 0 to 1 in red (matrix) and from -0.3 to 1 in green (disperse phases) was used. Therefore, this method is used in this project to compare between different polymers synthesized but not to compare them to other polymers whose data has not been processed the same way. Moreover, while in [15] only one measurement is presented, here at least three measurements were effectuated, showing the standard deviation some variability from one location to another. In agreement with [15] and [25], much phase segregation is detected for TPUs based on more aromatic isocyanates than for TPUs based on aliphatic isocyanates. This change can be attributed to a higher compatibility of the aliphatic long chain and the aliphatic hard segments [25].

Table 3.3: Microdomains percentual area coverage detected with FTIR mapping of the polymers based on one diisocyanate.

	Microdomains [%]
MDI-p	1.7 ± 0.6
HMDI-p	0.6 ± 0.5
PPDI-p	1.3 ± 0.3

3.2.4 Rheology

Temperature sweep analyses were performed in order to stablish the temperature corresponding to the network terminal relaxation, at the crossover between G' (storage module) and G'' (loss modulus), evaluating the dominance of viscous behaviour.

Figure 3.4 shows how HMDI-p starts already behaving like a viscous liquid at 38 ºC. This clearly limits the possible applications of the polymer. On the contrary, MDI-p and PPDI-p withstand much higher temperatures due to its aromatic structures. Moreover, while the loss modulus of PPDI-p only becomes larger than the storage modulus at 93 ºC, for MDI-p it occurs at much higher temperature, probably due to its double benzene structure.

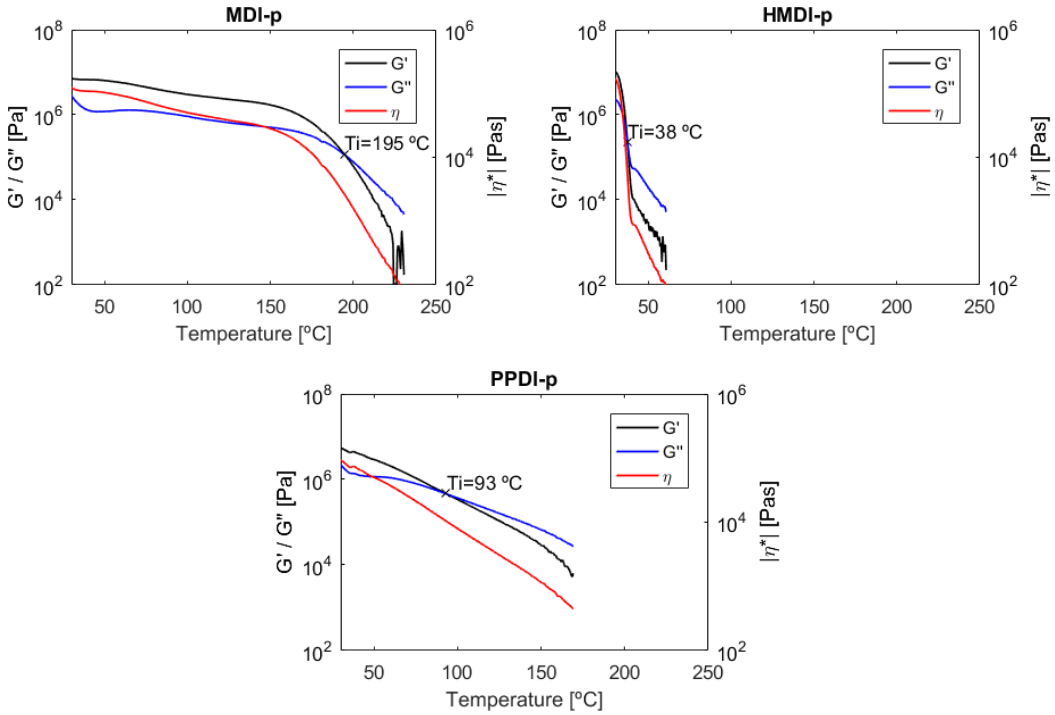

Figure 3.4: Rheology analysis for temperature sweep of MDI-p, HMDI-p and PPDI-p.

3.2.5 Fracture tests of pristine samples

Figure 3.5 shows the results for the fracture tests for samples MDI-p, HMDI-p and PPDI-p samples. HMDI-p exhibits a brittle behaviour and a higher slope load/displacement while MDI-p and PPDI-p show similar behaviour, allowing large deformations and reaching higher maximum strength than HMDI-p.

More thermoplastic behaviour is observed for the more segregated samples containing more aromatics in the hard block (MDI-p and PPDI-p), while more brittle behaviour corresponds to the least segregated with less aromatics (HMDI-p). As already confirmed in [16], better mechanical properties are observed in thermoplastic elastomers with good phase segregation such as MDI-p and PPDI-p. Furthermore, the lower hard segment weight percentage in the case of MDI-p and PPDI-p compared to HMDI-p leads to an increase in the maximum displacement and a decrease in the stiffness, as already stated in literature for tensile tests [25].

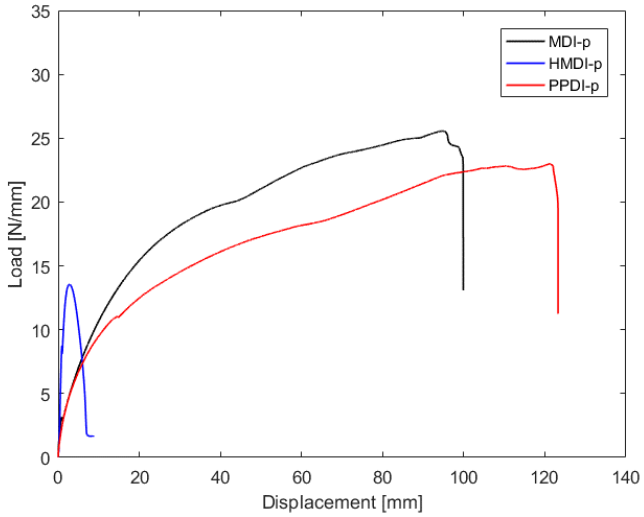

Figure 3.5: Representative load-displacement curve at 0.5 mm/s strain rate of the fracture tests showing the effect of the diisocyanate structure.

3.2.6 Healing characterization

As shown in Figure 3.6, HMDI-p shows almost no healing. Additionally, the results obtained for MDI-p and PPDI-p indicate that significant healing has been achieved considering the testing method is fracture. In the case of aromatic isocyanates, the aromatic interactions seem to play an important role in healing behaviour. In agreement with this, in [26], they demonstrated that polymers with aromatic interactions (π-π stacking) showed higher tensile modulus, toughness and healing properties than other healable materials. It should be noted that in all cases the facture surface obtained for the pristine samples, that was later healed, was always smooth, which enables the later healing and re-fracture and reduces differences between samples. After a sample had failed, nearly all deformation was recovered even before re-attaching the two parts of the sample. Some plastic deformation remained in the sample, what could be noticed by a slightly larger length dimension. This plastic deformation was almost inexistent for HMDI-p, as it can be observed in Figure 3.6.

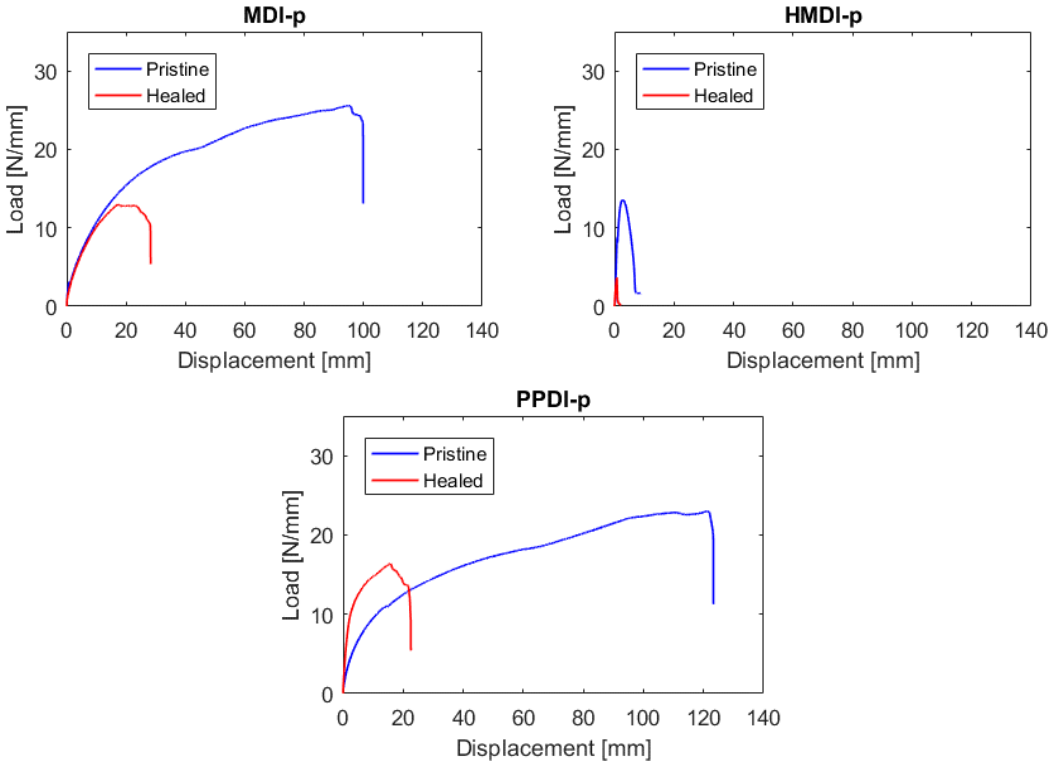

Figure 3.6: Representative load vs. displacement curve of the fracture tests for both pristine and healed MDI-p, HMDI-p and PPDI-p. Healing conditions 1 week at room temperature (22 ± 2 ºC) with no external pressure.

The healing efficiencies calculated for MDI-p, HMDI-p and PPDI-p are presented in Figure 3.7. The results obtained suggest that it is easier to heal strength than ductility. No error bars are displayed for PPDI-p as only one sample was tested. Although the error bars of HMDI-p may suggest higher healing for this polymer, it was clearly observed that re-attachment between both parts after failure was rather difficult. The fact that aromatic isocyanates present higher healing was not obvious, as normally higher healing efficiencies are expected for softer polymers as they have more mobility.

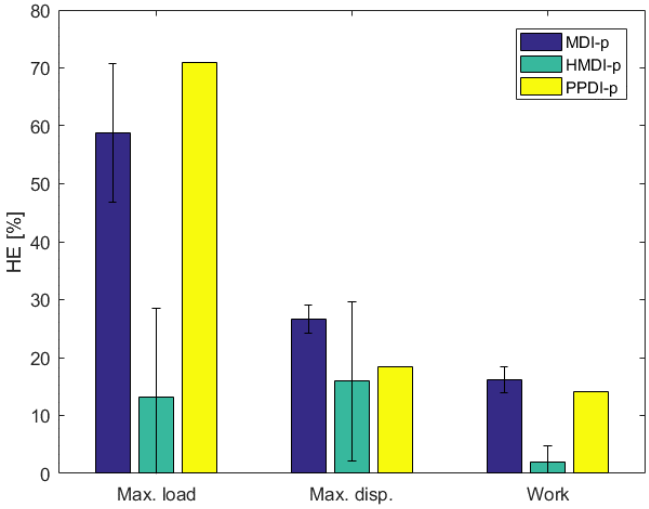

Figure 3.7: Healing efficiency for MDI-p, HMDI-p and PPDI-p according to maximum load, maximum displacement and work to failure. Healing conditions 1 week at room temperature (22 ± 2 ºC) with no external pressure Error bars are based on two repetitions except for PPDI-p where only one was tested.

In conclusion, the results advocate that the TPUs containing aromatic isocyanates (1) tend to have more micro-domains due to major incompatibility between hard and soft domains, (2) have better mechanical properties and (3) are capable of achieving higher healing efficiencies than cycloaliphatic isocyanates. However, the results do not clarify if the presence of micro-domains mainly detected in aromatic isocyanates can have a direct impact on the healing properties. This aspect will be addressed in chapter 5 with specific testing.

4 EFFECT OF THE COMBINATION OF ALIPHATIC AND/OR AROMATIC ISOCYANATES ON POLYURETHANE RANDOM COPOLYMERS

Above all, don't fear difficult moments. The best comes from them.

- Rita Levi-Montalcini-

According to the previous chapter, MDI-p and PPDI-p show significant healing efficiency at room temperature while HMDI-p does not. This is mainly attributed to the aromatic content of MDI-p and PPDI-p. However, HMDI-p has the advantage of low temperature terminal flow, which is favourable to achieve high healing efficiencies at moderated temperatures. Nevertheless, the quick transition to viscous flow at 38 ºC and the low mechanical properties and healing efficiency, restricts its applications and potential as a self-healing polyurethane. MDI-p and PPDI-p, in general, offer higher mechanical properties but also restricted motion at molecular level, what forces to heat the polymer up to 100 ºC to reach very high healing [15]. It is therefore presumed that mixtures of aromatic and aliphatic isocyanates and two sorts of aromatic monomers may lead to a good balance between mechanical properties, fast interfacial healing and high healing efficiency at long healing times and relatively mild temperatures. For this reason, this chapter explores the impact of isocyanate mixtures on the mechanical and healing behaviour of thermoplastic polyurethanes.

4.1 Polymer synthesis

In agreement with the polymer synthesis described in section 3.1, a molar ratio of 1:0.6 was used between CroHeal™ 2000 and EHD. 10 % mol excess of isocyanates was added with respect to the polyol mixture (CroHeal™ 2000 and EHD). Six different random copolymers were synthesized using two types of diisocyanates and varying the molar content of each diisocyanate (Table 4.1). The nomenclature used refers to the different isocyanates used (MDI, M; HMDI, H and PPDI, P) and to their molar composition; in this way, 'M80/H20' contains 80 % molar MDI and 20 % molar HMDI out of the total quantity determined for isocyanates. The homopolymers (which would correspond to M100, H100 and P100) were already studied in chapter 3 as MDI-p, HMDI-p and PPDI-p respectively.

All the polymers were synthesized in absence of solvent via one-shot technique in analogy to the process described in section 3.1. Nevertheless, some adjustments to the mixing protocol used in chapter 3 were implemented as shown in table 4.2 and described here below. The handling of CroHeal™ 2000, EHD, MDI, HMDI and PPDI was done as stated in chapter 3.

Table 4.1: Different polymers synthesised.

Polymer ID	Diisocyanate content
M80/H20	80% MDI + 20% HMDI
M60/H40	60% MDI + 40% HMDI
M40/H60	40% MDI + 60% HMDI
M80/P20	80% MDI + 20% PPDI
M60/P40	60% MDI + 40% PPDI
M40/P60	40% MDI + 60% PPDI

For M80/H20, M60/H40 and M40/H60, first MDI and, then, HMDI (already prepared in a syringe) were added to the polyol mixture on a scale to verify that the quantities added of isocyanates were accurate. MDI was added first to reduce its tendency to solidify in the cup. For M80/P20, M60/P40 and M40/P60, first PPDI was added followed by MDI to the polyol mixture on a scale. PPDI was first added due to its higher tendency to evaporate/solidify in the beaker. The order of addition of the diisocyanates was always the same, since it has been demonstrated that altering it could lead to significant changes [18].

Finally, and for all the polymer types, the cup was placed in a SpeedMixer™ DAC 400.2 VAC-P. The time in the speed mixer was modified for each TPU (Table 4.2) according to the reactivity of each isocyanate and the times already used in 3.1 Polymer synthesis. It should be highlighted that in all cases the time difference between pouring both diisocyanates was no more than a few seconds and that the cup with the mixture of polyol and isocyanates was quickly placed inside the SpeedMixer.

Table 4.2: Steps in the SpeedMixer™ for the different TPU.

	1st step - vacuum	2nd step – mixing – 2300 rpm
M80/H20	15 s	140 s
M60/H40		145 s
M40/H60		150 s
M80/P20		125 s
M60/P40		115 s
M40/P60		110 s

After mixing and for all the TPUs, the mixture was poured on PTFE moulds with dimensions 70 x 20 x 2.5 mm, covered with a PTFE slab with an aluminium plate with some weights on top and placed in the oven at 60 ºC for 24 hours to complete the reaction. The demoulding procedure was as described in 3.1 Polymer synthesis.

4.2 Results and discussion

4.2.1 Polymer synthesis

The MDI/PPDI random TPU copolymers showed more yellowing than MDI/HMDI copolymers (which were transparent) and signs of incomplete miscibility (Figure 4.3). This yellowing appearance is characteristic of the aromatic rings. Furthermore, bubbles tend to appear in the material, especially in the last part of material poured.

In the case of the fracture samples, small quantity of bubbles was detected (Figure 4.17) and always far from the fractured area.

Applying some pressure to the material when poured in the PTFE moulds was essential to achieve a homogeneous thickness. This constant thickness was desirable to conduct the rheology tests and it was crucial for the fracture tests. The MDI/HMDI random TPU copolymers were more easily poured than the MDI/PPDI ones. This can be attributed to the higher reactivity of the MDI and PPDI with respect to the HMDI.

The mass percentage of hard segments (HS) of all polymers is quite similar, as shown in Table 4.3, what reduces the impact of the ratio hard/soft segments when comparing the polymers.

Table 4.3: Hard segment percentage of the synthesized polymers with mixtures of isocyanates.

	HS [wt %]
M80/H20	21
M60/H40	21
M40/H60	21
M80/P20	20
M60/P40	19
M40/P60	18

4.2.2 FTIR

The FTIR spectra shown in Figure 4.1 and Figure 4.2 provides similar results for all polymers. However, some differences related to the aromatic/aliphatic structure of the diisocyanates as well as unreacted isocyanate in MDI/HMDI random copolymers can be noticed. The characteristic peaks of amide I, amide II, amide III, N=C=O and N-H, that allows to identify TPUs and to study the H bonding and the influence of the diisocyanate structure, have been marked in each of spectra.

The peak detected at 2262 cm^{-1} for MDI/HMDI copolymers in comparison to MDI/PPDI copolymers denotes the presence of unreacted isocyanate (N=C=O group). It should be noted how the intensity of the peak becomes higher as the content of HMDI increases. This indicates the lower reactivity associated with HMDI, as already observed in Figure 3.1. This problem is further addressed in 5.1.1.

The amide I band is normally localized around 1700-1740 cm^{-1} for diol extended polyurethanes [27] and it is mainly related to the carbonyl (C=O) stretching vibration and, in less percentage, to the C-N stretch [28][29]. Normally, the carbonyl peak for TPUs with different diisocyanates show small differences [16]. As it can be noticed in Figure 4.1 and Figure 4.2, all polymers have this peak in 1695-1696 cm^{-1}, similar to MDI-p and PPDI-p (Figure 3.1). The exception is the sample M40/H60, which has the peak at a lower frequency (1684 cm^{-1}), very similar to HMDI-p (1683 cm^{-1}, Figure 3.1).

The stretching vibrations of the N-H ranges from 3070 to 3500 cm^{-1}. The broad peak present in M80/H20, M80/P20, M60/P40 and M40/P60 at 3317 cm^{-1} and in M60/H40 and M40/H60 at 3325 cm^{-1} denotes the presence of N-H bonds in the urethane linkage.

Amide I band and N-H band tend to shift to lower frequencies with the formation of H bonds [27]. The vibration of free N-H varies from 3300 to 3500 cm^{-1} while the H bonded N-H varies from 3070 to 3350 cm^{-1} [29]. Although in this case, the frequency of 3317 cm^{-1} and 3325 cm^{-1} cannot directly be attributed to N-H H bonded, the fact that amide I is shifted to lower frequencies (1695 cm^{-1} against the normal 1700-1740 cm^{-1}), denotes that H bonding interactions are formed (N-H…O=C). Furthermore, the fact that this peak is very close to 3350 cm^{-1} denotes stronger H bonds.

Yilgor et al stated in [16] that urethane groups with medium to strong hydrogen bonds have their amide I peak at 1695 cm^{-1}, what coincides with the obtained results, except for M40/H60. Additionally, they also compared

urethane compounds based on HMDI, obtaining a lower peak at 1685 cm^{-1}, similar to H40/H60. They attributed this lower peak to the well-ordered structure of the H bonds present in HMDI based urethane compounds [16].

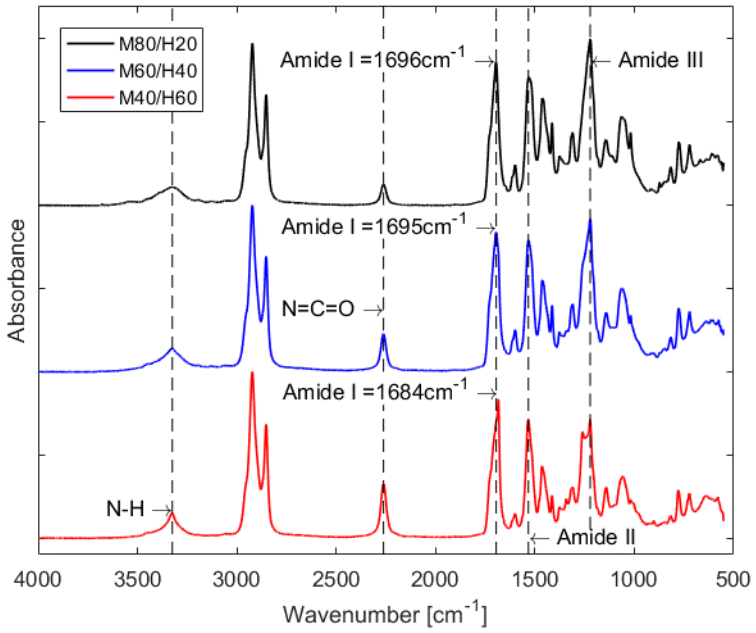

Figure 4.1: FTIR analysis of the MDI/HMDI TPUs.

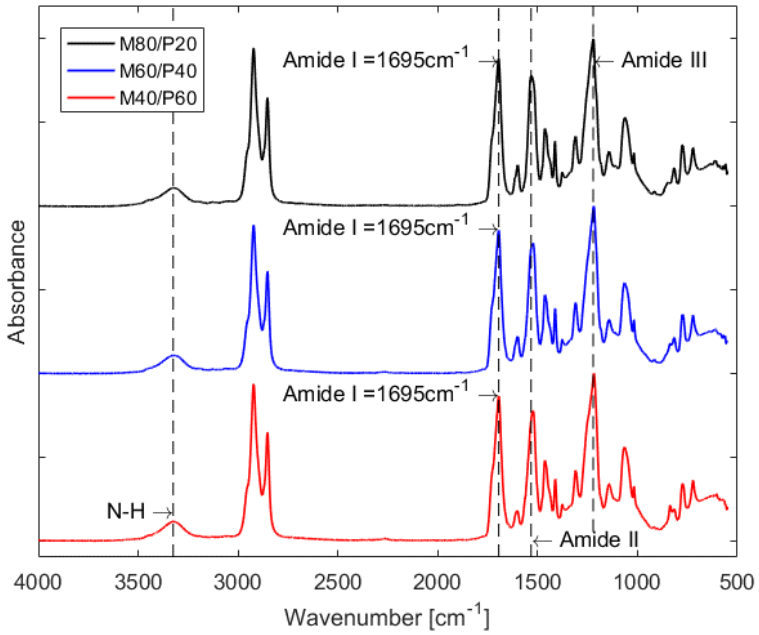

Figure 4.2: FTIR analysis of the MDI/PPDI TPUs.

The amide II and amide III bands are normally used in polyurethanes to prove the formation of the urethane bonds and H bond [30]. The amide II band is situated around 1530-1540 cm^{-1} and it is principally associated to the C-N stretching, N-H bending and also to the CCC deformation vibrations [27][29][30][31]. M80/H20, M60/H40, M40/H60 and M80/P20 have the amide II peak located in 1533 cm^{-1} while M60/P40 and M40/P60 have it in 1525 cm^{-1}. The amide III band is normally found in 1220-1230 cm^{-1} and it is assigned to the C-N-H deformation and the C-N and C-C stretching [29][27][30]. For M80/H20, M60/H40, M40/H60 and M80/P20 this amide III is situated at 1222 cm^{-1}. For M60/P40 and M40/P60, it is slightly shifted to the right to 1219 and 1218 cm^{-1} respectively.

In previous studies of polyurethane soft and hard segments [27], it has been shown that the H bonding interaction can be formed by NH…O=C (Type I) for hard segments and by NH…O (Type II) in soft segments. The amide II band is mainly associated to the Type II H bonds in the soft segments while the amide III band is more related

to the Type I. The amide I band as well as N-H stretching are mainly related to Type I H bonds [27].

In general, the amide II peak associated to soft segments (SS) is found at higher wavelengths than those reported in literature while the opposite is detected for amide III [27]. In this case, the peaks of M60/P40 and M40/P60 have shifted to lower frequencies and, therefore, it cannot be attributed to a larger effect of the hard segments (HS). As these two polymers were the ones showing more miscibility problems, the shifts in frequencies can be related to it.

The frequencies between 1300 and 1500 cm^{-1} refer to CH and CH_3 deformation vibrations while bands between 1000 and 1200 cm^{-1} are related to the CH_3 rocking vibrations [29], mainly related to the long chain polyol. Furthermore, the higher peak at 2922 cm^{-1} of M60/H40 and M40/H60, associated to CH_2, denotes the influence of the aliphatic character of HMDI [30].

4.2.2.1 Miscibility problems detected in M80/P20, M60/P40 and M40/P60

As mentioned in 4.2.1 Polymer synthesis, when the thermoplastic polyurethanes made with mixtures of MDI and PPDI were synthesized, it could be clearly distinguished some yellow areas non-uniformly distributed in the samples. Figure 4.3 shows one of these areas. It should be noticed that, in general, these areas were rather smaller (around 2-3 mm) than the one shown in Figure 4.3 and mainly present in M60/P40 and M40/P60. This image was used for ease of visualization and not to characterize the dimensions of these macro-phases.

When these areas were analysed, the IR spectrometer revealed that they had the same composition as the rest of the sample except for a noticeable peak at 2262 cm^{-1} (Figure 4.4). This specific wavelength, as previously discussed, refers to the group N=C=O and indicates the presence of unreacted isocyanate. The IR signal for this peak is larger for M80/P20, then for M60/P40 and, finally, for M40/P60. The segregation observed in these samples can denote certain degree of incompatibility between the two aromatics. Another factor that strongly influences the appearance of this segregation is the high tendency of the isocyanate PPDI to form crystals when heating and to solidify while pouring it into the mixture of polyol and chain extender.

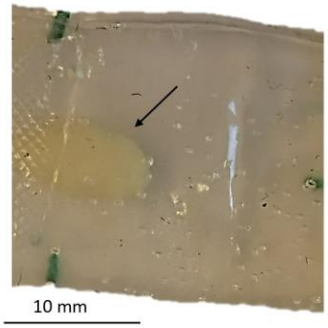

Figure 4.3: Yellowish areas observed in TPUs with mixtures of MDI and PPDI

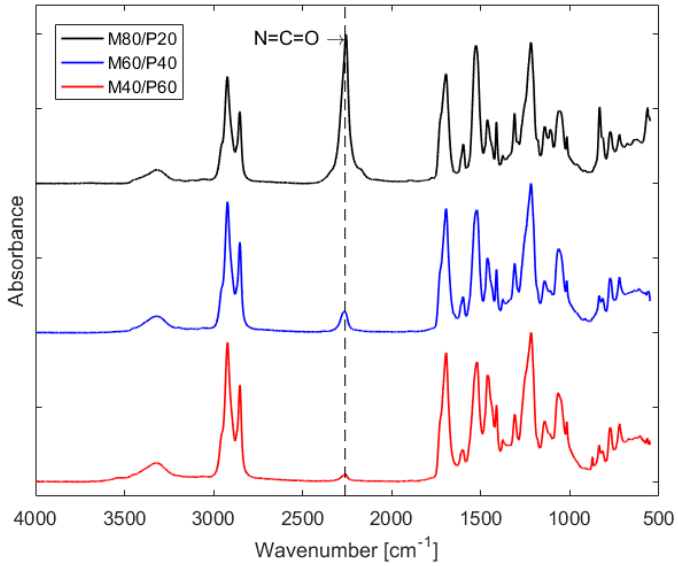

Figure 4.4: FTIR analysis of the MDI/PPDI TPUs random copolymers for yellowish areas.

4.2.3 TGA

The TGA was used to exclude any possible degradation of the polymer during any characterization method or during its processing. The results obtained from the TGA are shown in Figure 4.5 and the degradation temperatures (T_d) considering a 2 % weight loss, the temperature with highest decomposition rate ($T_{d,max}$) and the temperature onset of the second stage observed in the graphs ($T_{d,HS}$) are detailed in Table 4.4. The two-step curve obtained suggests the polymers are segmented polyurethanes.

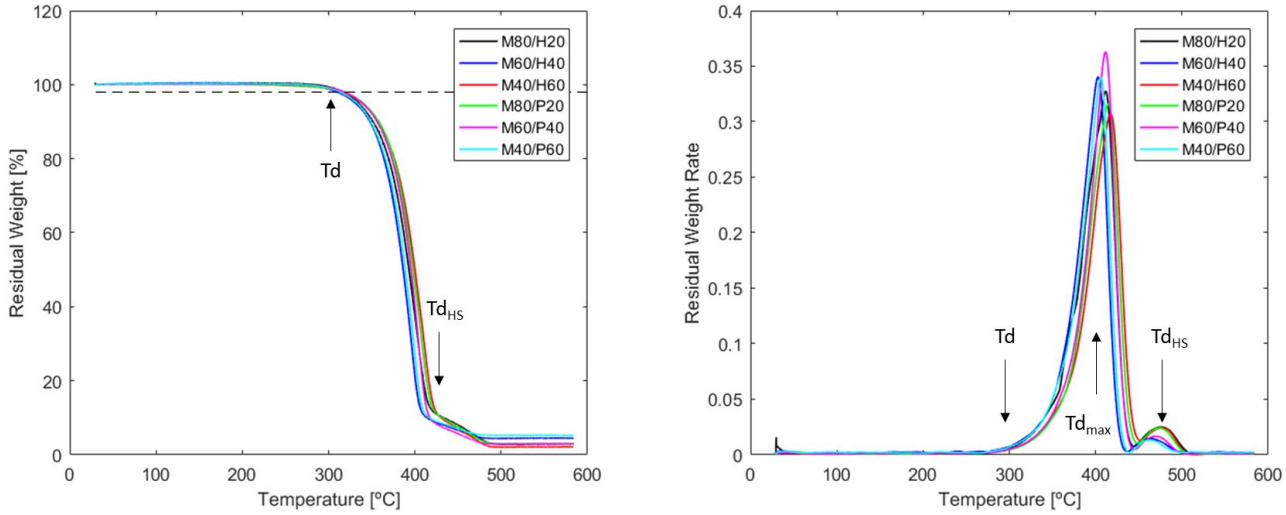

Figure 4.5: TGA results: on the left, evolution of percentage of residual weight with temperature marking with dotted line the 2% weight loss and, on the right, derivative of the residual weight.

Table 4.4: Degradation temperature of the six TPUs.

	Td [ºC]	**Td_{max} [ºC]**	**Td_{HS} [ºC]**
M80/H20	317	412	444
M60/H40	310	403	436
M40/H60	315	417	452
M80/P20	317	415	447
M60/P40	319	412	445
M40/P60	313	406	439

The degradation temperatures of all the polymers are similar, varying from 310 ºC to 320 ºC and, therefore, showing high thermal stability. No clear tendencies are observed in relation to the composition of the TPUs. Polyurethanes are generally considered to be thermally unstable due to the urethane groups, which start degrading at 150 ºC – 210 ºC depending on the polyol, chain extender and isocyanate used [32][33]. Nevertheless, in this case, the polyurethanes synthesized are more thermally stable and do not start degrading until 260 ºC, as it can be observed in Figure 4.5, in the derivative of the weight loss. This can be due to the fact that in a segmented polyurethane, the thermal stability is not necessarily determined by the weakest bond but by the most frequently occurring one. The thermal stability of segmented polyurethanes depends on the length of the segments and their concentration [33]. Therefore, as the HS structure and concentration is similar for M80/H20 and M80/P20 (i.e. larger presence of MDI) similar results are obtained.

From the residual weight curve and its derivative, it can be easily observed two clear stages in the degradation, as it is typical in polyurethanes [34][35][36]. The first drop in weight can be related to the SS as they represent a larger weight percentage in the network in comparison to the HS and, therefore, the higher weight loss percentage. The second weight loss can be connected to the degradation of the hard segments, present in less

quantity. The fact of having stronger interaction within the hard blocks also contributes to more thermal stability. An initial degradation temperature of the HS is found around 440 ºC for all polymers. No clear difference according to the type of isocyanate is observed. The differences observed between different TPUs can be attributed to a matter of deviation.

4.2.4 DSC

Figure 4.6 shows that only one glass transition temperature (T_g) is detected which is associated to the soft segments. As stated in [37][38], the heat flow variation during the T_g of hard blocks is very small and almost undetectable by the DSC. Figure 4.7 represents the first and second cooling curves where no exothermic peak related to crystallization is found. The heat absorption for M40/H60 (observed in both Figure 4.6 and Figure 4.7) is slightly different when compared to the rest, this can be attributed to possible bending of the cup containing M40/H60 and, therefore, more heat needed to heat up the sample.

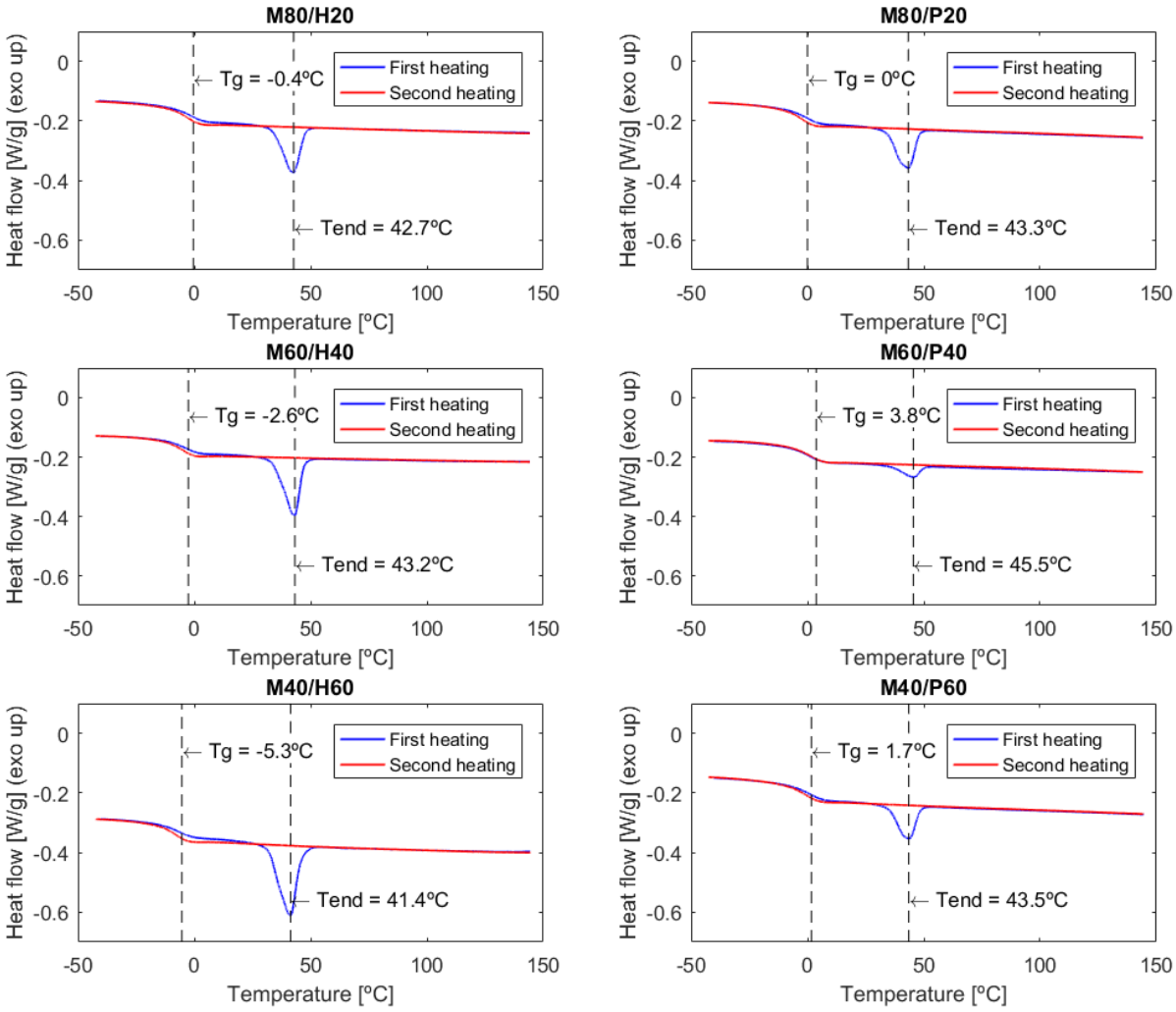

Figure 4.6: DSC heating curves marking the glass transition temperature (T_g) and the endothermic peak (T_{end}) of each copolymer.

The T_g has been calculated as the maximum of the derivative of the heat flow for the second heating curve. As expected, the TPUs with a larger content of aliphatic chains (HMDI) are characterised by lower T_g due to their increased mobility. The fact that MDI has a CH_2 between the two benzenes provides more flexibility to the network in comparison to PPDI and, therefore, higher T_g is obtained for MDI/PPDI copolymers with larger percentage of PPDI. Thus, the increased number of aromatic rings of M80/H20 seems to have less influence on the reduction of flexibility than the CH_2 linkage between benzenes.

There is a clear difference between the first heating curve and the second heating curve: an endothermic peak around 40-50 ºC. This thermal transition can be attributed to the relief of stresses created during the demoulding process as the thermal variation that the polymer is subjected to is more than 40 ºC. The endothermic peak can

also be associated to the melting of the unreacted isocyanate. This way, it can be observed that the samples which present higher percentage of this unreacted isocyanate (in decreasing order M40/H60, M60/H40, M80/H20, M80/P20, M40/P60 and M60/P40) show a more pronounced peak. In other studies with TPUs [39], endothermic peaks in the range of 20 ºC were related to the melting and, therefore, crystallinity of the soft segments. They concluded the melting peak was related to the soft segments as both the polymers with and without chain extender showed this peak. Another possibility is the melting of the physical crosslinking of the HS, related to the crystallinity of these areas, which allows the TPUs to be moulded or extruded [11]. These hypotheses are further discussed in 5.1.3 Thermal transitions.

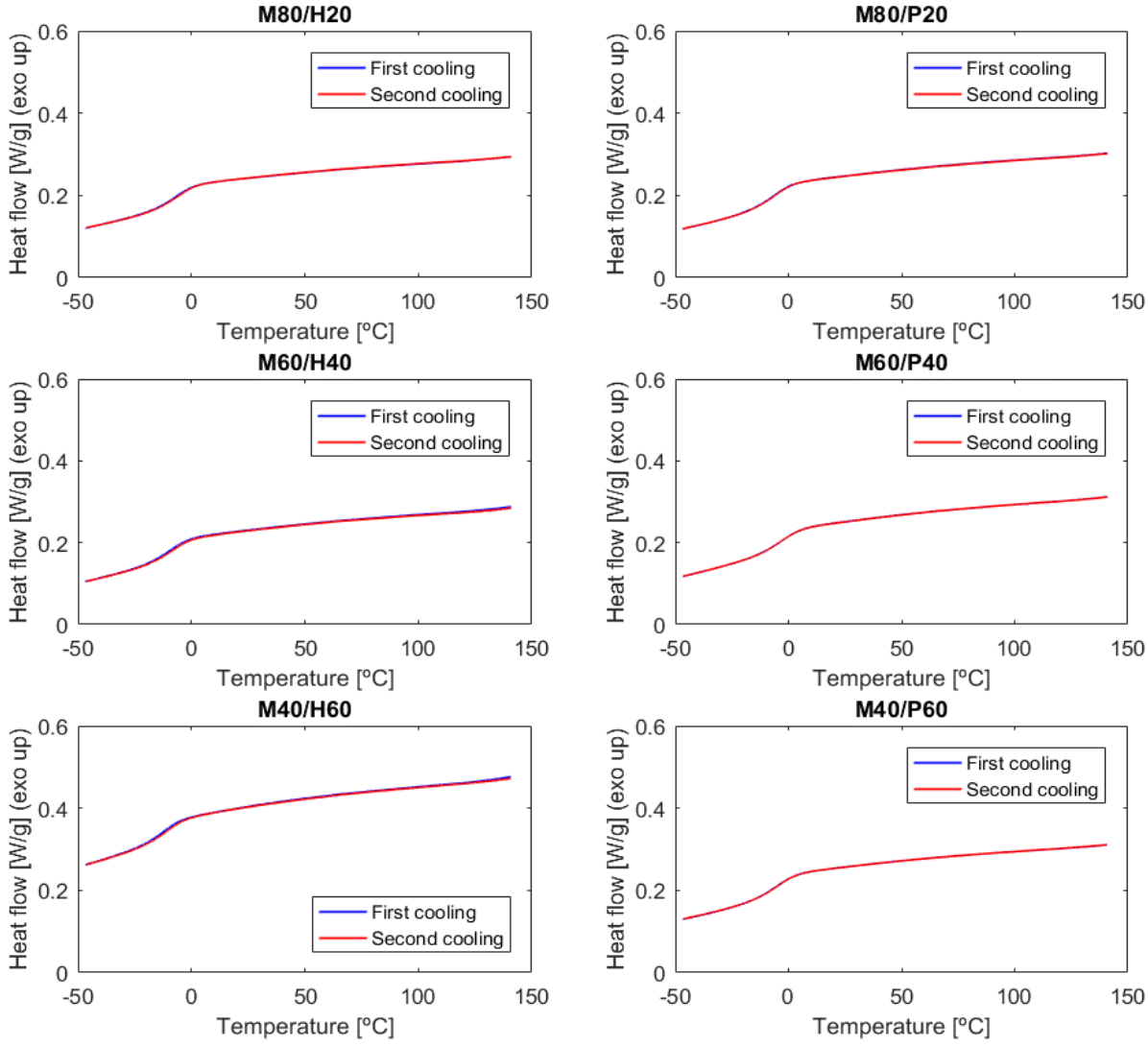

Figure 4.7: DSC cooling curves for each copolymer.

4.2.5 FTIR mapping

The segmentation of TPUs into hard and soft segments has been extensively studied to determine the structure properties of the resultant copolymers. The hydrogen bonding and/or crystallization formed between the dispersed hard segments act as pseudo crosslinks [40]. The phenomenon of segmentation has been previously demonstrated by small-angle x-ray scattering, by SEM, by pulsed nuclear magnetic resonance, by observation of the mechanical properties (e.g. dynamical mechanical analysis) and by calorimetry [11][37][41]. The phase separation into hard domains and soft domains is normally incomplete, having the hard domains certain quantity of soft domains and vice versa. The average size of these domains ranges from 10 to 20 nm increasing with the HS content. The morphology of the hard domains varies from long needles 50-300 nm long and 5 nm thick to spheres of 5-20 mm diameter [11].

In the present work, micro-phase segregation is observed with the use of an ATR-FTIR microscope and a principal component analysis. It should be highlighted that this micro-phase segregation is not directly related to hard domains and soft domains, observed in the nm scale, but to the larger concentration of one of them, as explained in Figure 1.2. This way, the micro-domains or disperse phases are characterised by a higher presence of HS and the matrix, by a higher concentration of SS.

The analysis is based on local differences on composition detected with the FTIR mapping. Figure 4.8 displays one of the ATR images obtained for each of the six TPUs copolymers while the rest can be consulted in the appendix (Figure A.5). M80/H20 and M60/H40 are the ones which exhibit more dispersed phases (green areas) in the matrix (red areas). Table 4.5 collects the results for the average percentage of disperse phases obtained for at least three images per type of polymer and Figure 4.9 represents this data according to the TPU composition (MDI-p, HMDI-p and PPDI-p have been added for completion). M60/P40 and M40/P60 show a very large deviation, what is mainly attributed to the miscibility issues already discussed in 4.2.2.1.

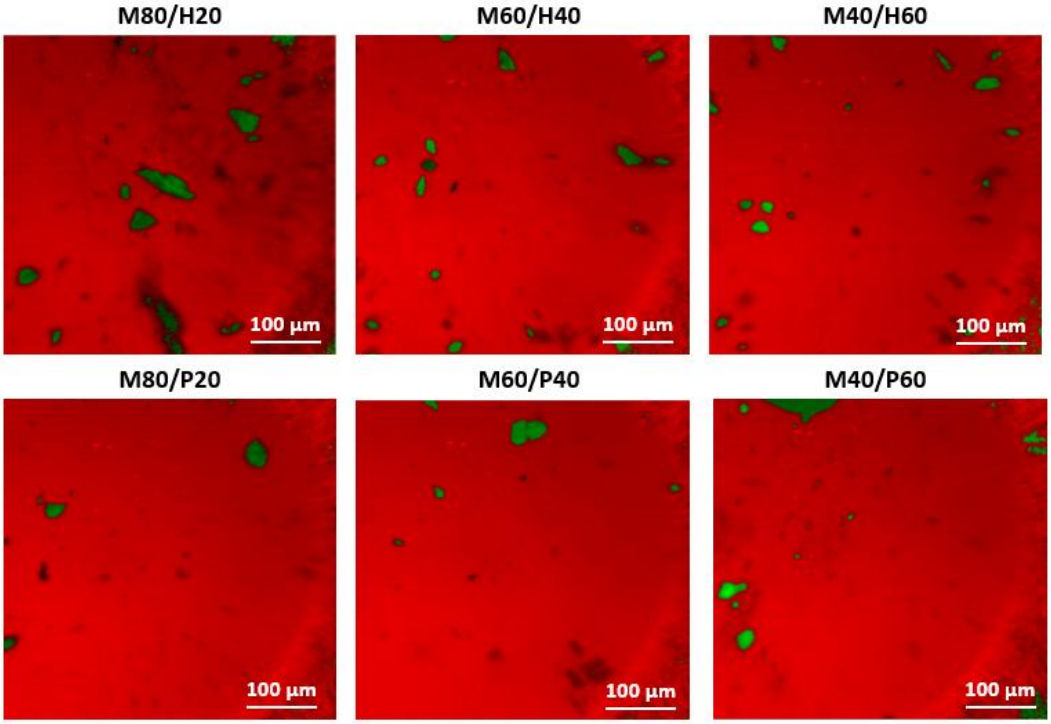

Figure 4.8: FTIR mapping-image of all the polyurethanes synthesized (on the surface of the samples) showing the micro-domains (green) and the matrix (red).

Table 4.5: Microdomains percentual area coverage detected with FTIR mapping of the polymers based on mixtures of diisocyanates.

	Microdomains [%]
M80/H20	2.8 ± 0.7
M60/H40	2.3 ± 0.7
M40/H60	1.3 ± 0.4
M80/P20	0.9 ± 0.5
M60/P40	2.2 ± 2.0
M40/P60	2.1 ± 2.7

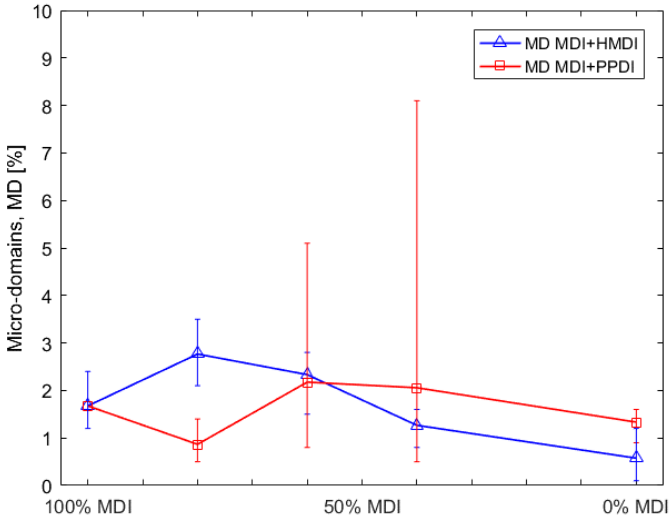

Figure 4.9: Microdomains average percentage detected with FTIR mapping of the polymers based on mixtures of diisocyanates. Error bars representing the minimum and the maximum value obtained for each TPUs.

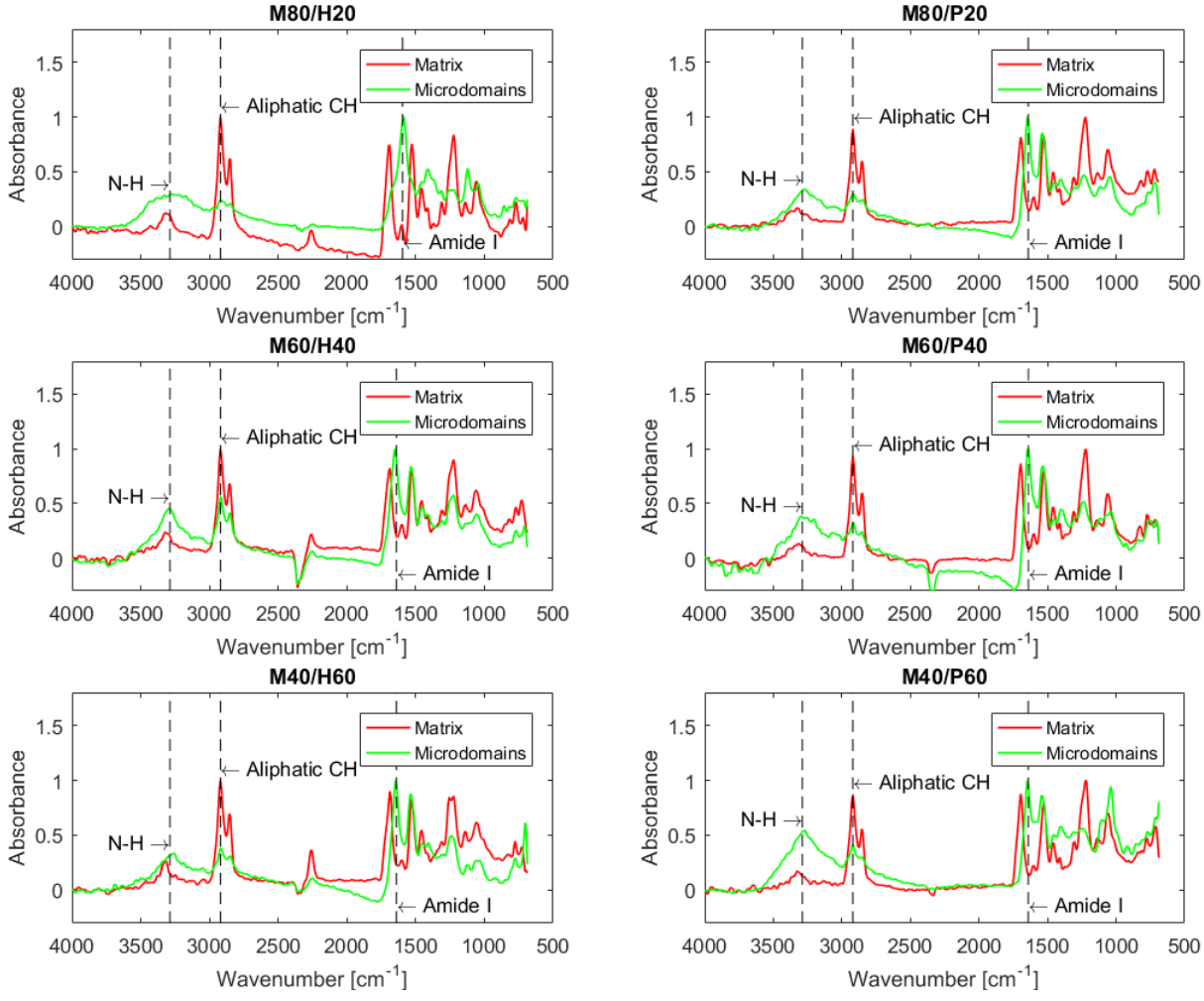

Figure 4.10: FTIR-ATR spectrum of all the polyurethanes synthesized distinguishing between matrix (red) and micro-domains (green).

IR analysis indicates there are two governing compositions related to the matrix and the phases as shown in Figure 4.10. It is common in all polymers that a stronger absorption for N-H stretching and amide I are present for the disperse phases, groups typically found in hard domains. Furthermore, the amide I peak, and the N-H stretching is shifted to lower frequencies in the disperse phases, what denotes the existence of stronger H bonds. Indeed, in homopolyurethanes synthesized from only chain extender and diisocyanate (main constituent of HS),

the presence of H bonds is larger than in the homopolymers synthesized from only polyol and diisocyanate (main constituent of SS) [11]. In the matrix, a higher peak in 2920 cm^{-1} is found, which is related to asymmetric stretching of CH_2 and outlines the predominance of soft domains from the long and branched polyol [31]. For the MDI/HMDI copolymers, it should be highlighted that the unreacted isocyanate already detected with the FTIR is only detected in the matrix. Therefore, unreacted isocyanate tends to appear in soft segments rather than in hard segments. Figure 4.11 shows the different characteristic peaks of PUs for matrix and microdomains, already discussed in 4.2.2 FTIR. As already mentioned, it can be easily observed the lower frequencies of amide I and the higher frequencies of amide II for the disperse phases.

The spectra obtained for the microdomains of M80/H20 is slightly different from the others as no peak but a shoulder is detected at 1536 cm^{-1} for amide II and the amide I peak is shifted to 1595 cm^{-1} (1640 cm^{-1} for the rest). The other most similar compositions (M80/P20 and MDI-p) show a clear peak and no shoulder. In the previous section 4.2.2 FTIR, the amide II has been mainly related to the SS; therefore, the disappearance of this peak can be related to a stronger concentration of HS in the disperse phases detected. Moreover, the shift of amide I to lower wavelengths can hinder the visibility of this peak.

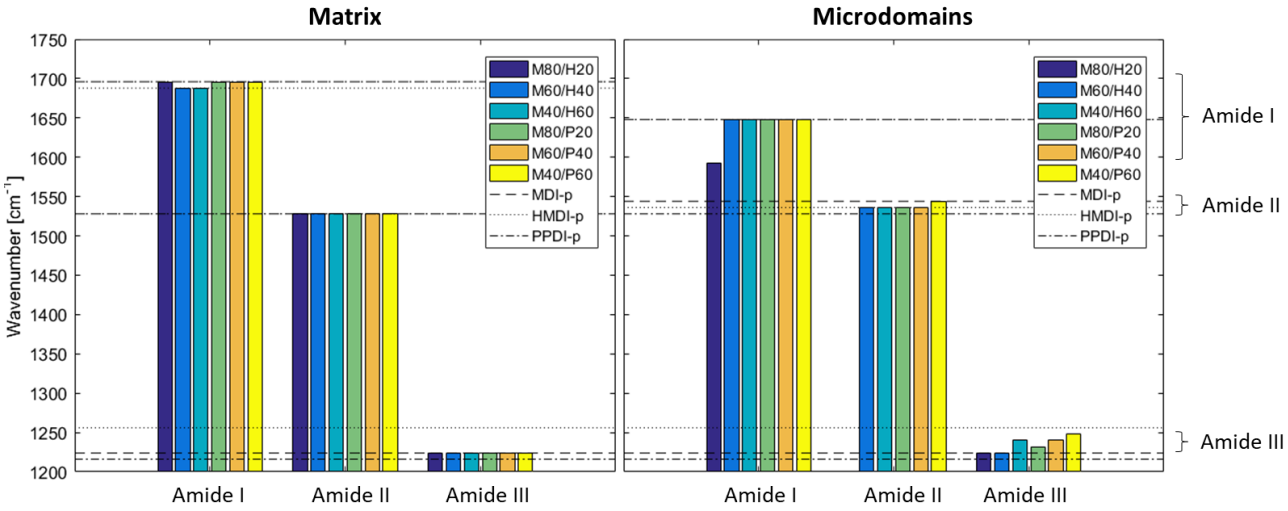

Figure 4.11: Values of the different representative peaks obtained for both matrix and microdomains for all polymers.

4.2.6 Rheology

Figure 4.12 displays the temperature sweep results obtained for the six TPUs synthesized. In all graphs the cross point between the viscous modulus (G'') and the elastic modulus (G') has been included. Above the crossover the polymer starts behaving more like a viscous liquid. Therefore, the mobility of the network is higher as the molecular interactions are lower, facilitating interchain diffusion and randomization.

The rigidity of the polyurethane network decreases in the order aromatic > cycloaliphatic > aliphatic [20], this translates into higher crossover temperature and T_g for polyurethanes based on aromatics. In the results, it is clear how the cycloaliphatic chain present in HMDI provides more mobility to the network and, therefore, polymers with larger percentage of HMDI show a lower crossover temperature. Moreover, polymers with more content of HMDI show a more pronounced drop in the complex viscosity.

It is highly interesting how for MDI-p the cross point is located at 195 ºC and for HMDI-p, at 38 ºC (Figure 3.4), and when only 20 % of HMDI is added in the synthesis, this value sharply drops to 52 ºC. The increased mobility of the new created network suggests that M80/H20 would be able to achieve higher healing efficiencies at moderate temperatures for long times than MDI-p. For short times less healing would be expected as in principle fast healing is related to aromatics, as suggested in 3.2.6 and concluded in [42].

Regarding M80/P20, M60/P40 and M40/P60, the results show no clear tendency. This can be related to the difficulty to synthesize these polyurethanes and the lack of homogeneity shown in the final samples as discussed in 4.2.2.1. M80/P20 shows lower crossover than M60/P40 and M40/P60 due to its lager content of MDI. This is explained due to the CH_2 present between the two benzenes in the case of MDI, which provides more flexibility to the structure (as discussed in 4.2.4 for the DSC results).

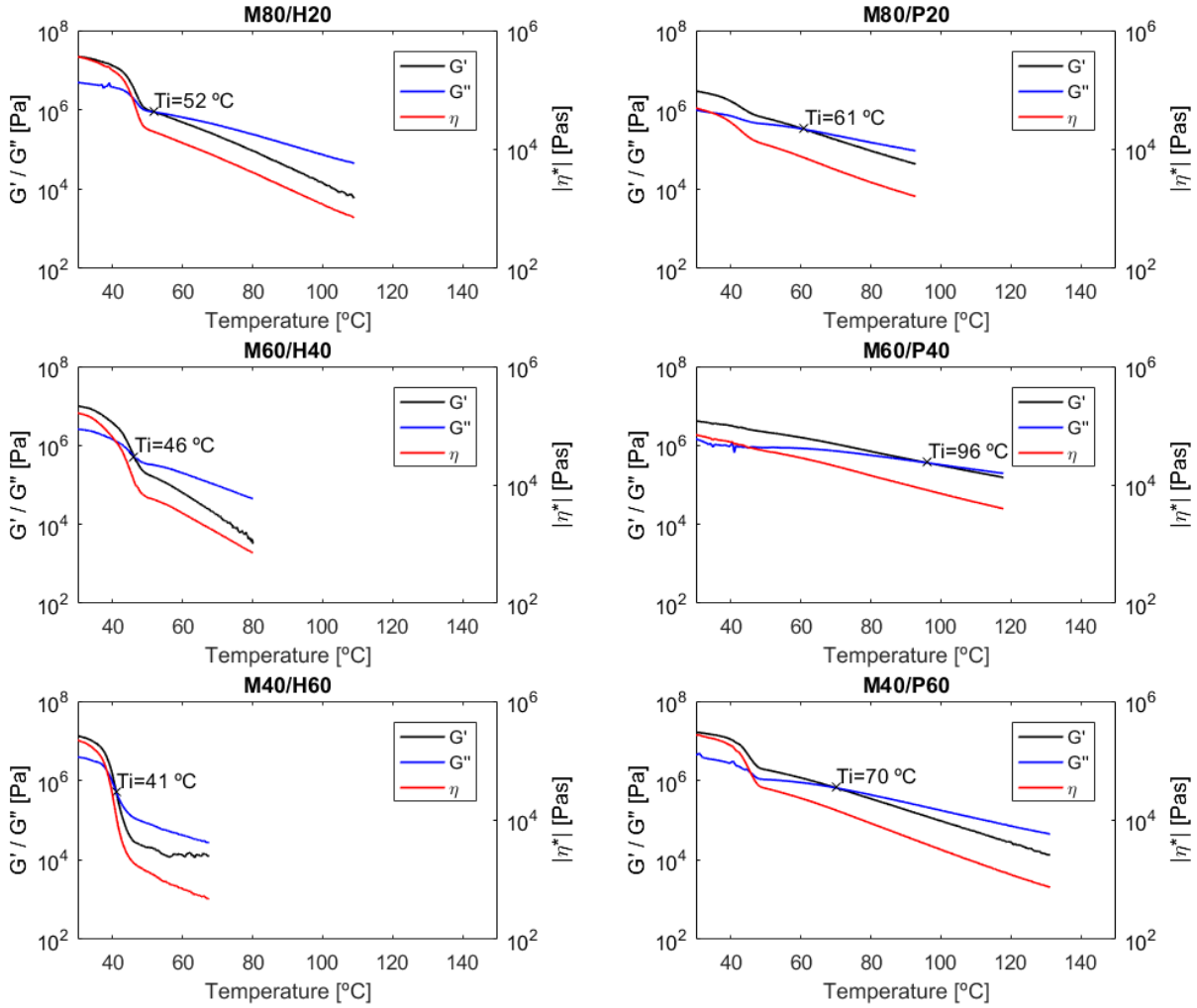

Figure 4.12: Temperature sweep rheology for all polymers.

4.2.7 Fracture tests of pristine samples

In order to characterize the mechanical behaviour and, ultimately, the healing efficiency of the polymers synthesized, fracture tests were conducted with a crosshead speed of 0.5 mm/s at 10 ºC, which is above the T_g for all polymers according to DSC results. In Figure 4.13, the load-displacement curves for all samples is presented. It should be noted that since not all the samples have the same thickness, the load has been divided by the thickness, as it is normally performed in plane stress conditions. In all cases, the initial load was followed by notch blunting and crack propagation perpendicular to the direction of the load applied.

Polymers with larger content of HMDI are characterized by a stiffer response and smaller plastic deformation. Additionally, larger percentages of aromatic diisocyanates (MDI and PPDI) provide less stiffness and more plasticity, as their benzene groups allow larger deformation without failure. Therefore, the use cycloaliphatic isocyanates results in a more brittle structure, more characteristic of non-segmented thermoplastics, while aromatic isocyanates give more ductility, more identified with the typical segmented elastomeric behaviour. The peak that can be distinguished in M80/H20 and M80/P20 can be attributed to a partial healing of the pre-notch during the clamping procedure.

The polyurethanes showing larger work to failure are M80/H20, M80/P20 and M40/P60. This confirms one more time how the aromatic character of MDI and PPDI provides less mobility in the polymeric network and, therefore, higher mechanical properties.

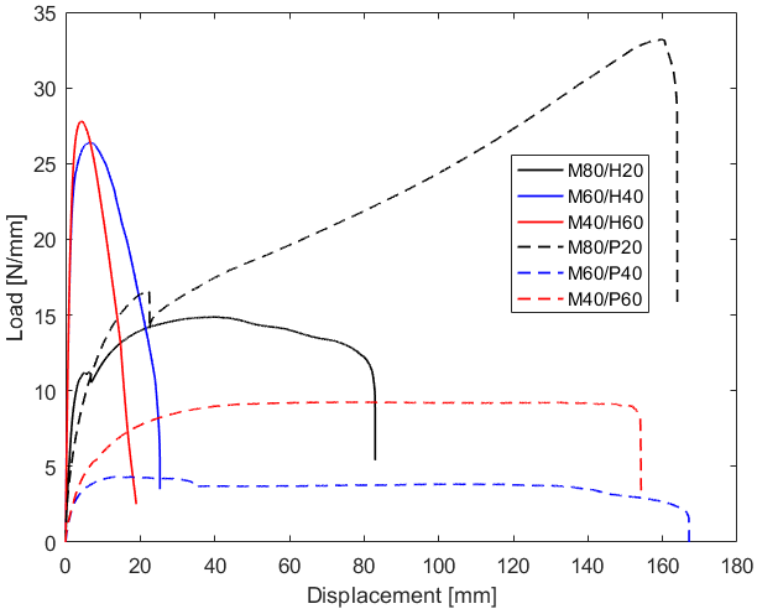

Figure 4.13: Representative load-displacement curve at 0.5 mm/s strain rate of the fracture tests showing the effect of diisocyanate mixtures. MDI/HMDI TPUs with solid line and MDI/PPDI with dashed line.

4.2.8 Healing characterization

The ideal self-healing material would have high mechanical properties while it would be able to heal at low temperatures. However, the reformation of the H bonds in TPUs requires molecular mobility and high mechanical properties and mobility are contradictory and hard to be accomplished simultaneously [8][6]. Although it has already been demonstrated that the mechanical response of supramolecular elastomers is sensitive to strain rate (decreasing load and increasing deformation when strain rate is decreased), the healing efficiency has been demonstrated mainly independent [5], what makes the results shown in this section highly valuable for future applications.

As previously studied, MDI-p and PPDI-p possess high mechanical properties. Moreover, although HMDI-p has lower mechanical properties, it also flows at much lower temperatures and so do the polymers combining MDI and HMDI, as demonstrated in 4.2.6 with rheology. This is advantageous from the point of view of the mobility required for healing and suggests that higher HE can be achieved for low temperatures.

In order to confirm the previous hypothesis, M80/H20, M60/H40, M40/H60 and M80/P20 were healed for 1 week at room temperature and, then, re-fractured. The healing procedure for M60/P40 and M40/P60 was not possible due to the large plastic deformation in the interface and the absence of a smooth interface in contrast with the rest of the samples.

Figure 4.14 depicts the results for the pristine and healed samples. It can be observed that it is easier to heal strength than plasticity, as it is displayed in Figure 4.15. This is expected due to the memory effect of the material as these samples have been previously loaded, afterwards healed and, finally, loaded again. Therefore, plastic deformation remains in the sample. In [42], Susa et al also observed how the restoration of the mechanical strength was easier than the restoration of the plastic deformation in polyimides. The most unexpected case is the one of M80/H20 where the maximum strength is increased above the maximum strength experienced in the pristine sample. This phenomenon would be analysed in the next chapter, in section 5.2. All cases have been repeated twice confirming the data obtained.

Figure 4.15 gather the information regarding the healing efficiency. The highest HE, calculated as the average of two samples, is obtained for M80/H20 followed by M60/H40, M80/P20 and M40/H60 in decreasing order. Although the HE for M80/P20 is not as high as for M80/H20, the mechanical properties of the healed samples remain being the best amongst all. In general, it is shown that even though aromatic diisocyanates allow less mobility, they also provide higher healing. When comparing the data from MDI-p (Figure 3.7) and M80/H20 (Figure 4.15), it can be concluded that the higher flexibility provided by the HMDI results beneficial for the healing, as higher HE based on work to failure is obtained. For the case of M80/P20 and MDI-p, similar results are obtained.

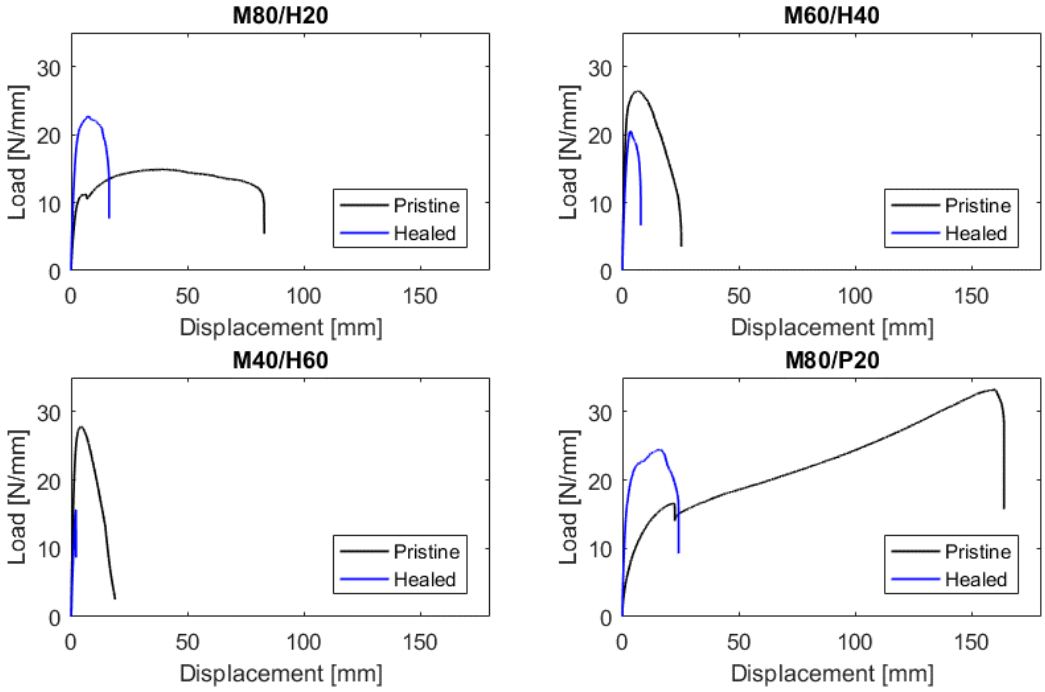

Figure 4.14: Representative load vs. displacement curve of the fracture tests for both healed and pristine samples. Healing conditions 1 week at room temperature (22 ± 2 ºC) with no external pressure.

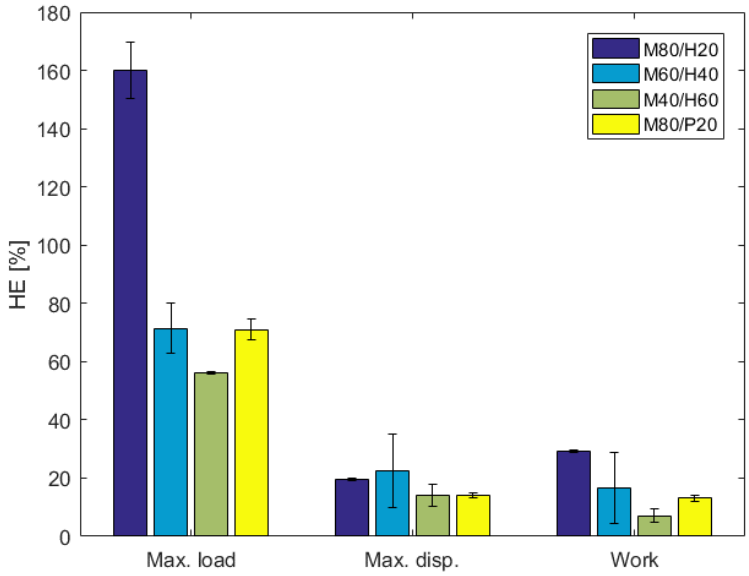

Figure 4.15: Healing efficiency of M80/H20, M60/H40, M40/H60 and M60/H20 according to maximum load, maximum displacement and work to failure. Healing conditions 1 week at room temperature (22 ± 2 ºC) with no external pressure Error bars are based on two repetitions.

One advantage of intrinsic self-healing materials against extrinsic self-healing materials is their possibility to theoretically heal an indefinite number of times. In order to assess the ability of the samples to heal a second time, another fracture test was performed again one week after the previous one. This test was not possible for M60/H40 and M40/H60 as due to their reduced ability to heal, it was not possible to reattach both parts after the first damage-healing-damage cycle.

As it can be noticed in Figure 4.16, the mechanical properties in the second healing are reduced and no further increment in strength is experienced. In this case, the healing efficiency with respect to the pristine work to failure ($HE_{pristine}$) and with respect to the first healing ($HE_{1^{st}\ healing}$) is higher for M80/P20 (Table 4.6). This is expected due to the larger content of aromatics present in M80/P20. All the results presented in Figure 4.14 and Figure 4.16 can be confirmed with Figure 4.17, where it is clear how the samples start loosing ductility when healing is conducted. It should be underlined how the crack always propagates in the same place, not diverting

its path from the middle plane of the sample, perpendicular to the tensile direction. Moreover, it has been confirmed that crack propagation observed in fracture tests provides information regarding the relation between the mechanical properties and the polymer structure [5]. In this case, it can be observed from the photos that the polymer structure shows an elastomeric character for M80/H20 and for M80/P20 while M60/H40 and M40/H60 present the typical thermoplastic behaviour.

Considering the rheology results for the temperature sweep (Figure 4.12), it can be speculated that at higher temperatures (~ 50-60 ºC) interphase healing would take place being able to heal multiple times achieving high HE.

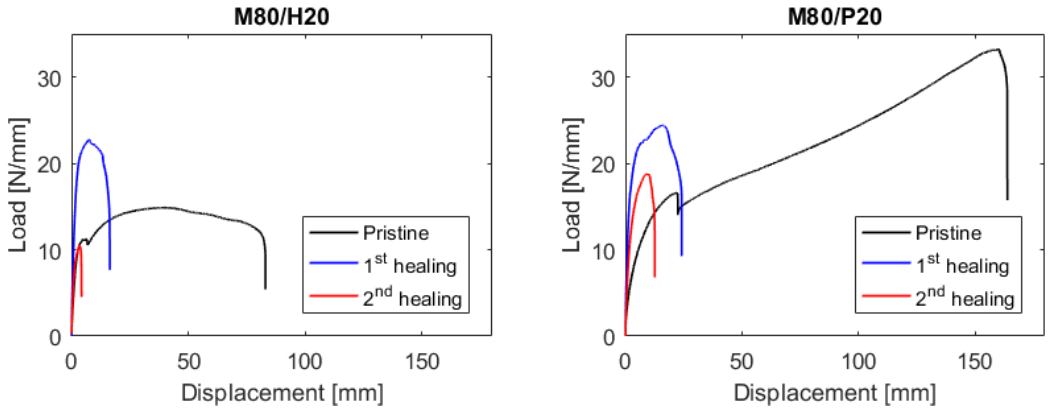

Figure 4.16: Load vs. displacement curve of the fracture tests for samples healed twice. Healing conditions 1 week at room temperature (22 ± 2 ºC) with no external pressure.

Table 4.6: Healing efficiency for the second healing in comparison to the pristine sample ($HE_{pristine}$) and to the sample healed one ($HE_{1^{st}\,healing}$) for healing conditions: 1 week and RT.

	$HE_{pristine}$ [%]	$HE_{1^{st}\,healing}$ [%]
M80/H20	4	13
M80/P20	5	35

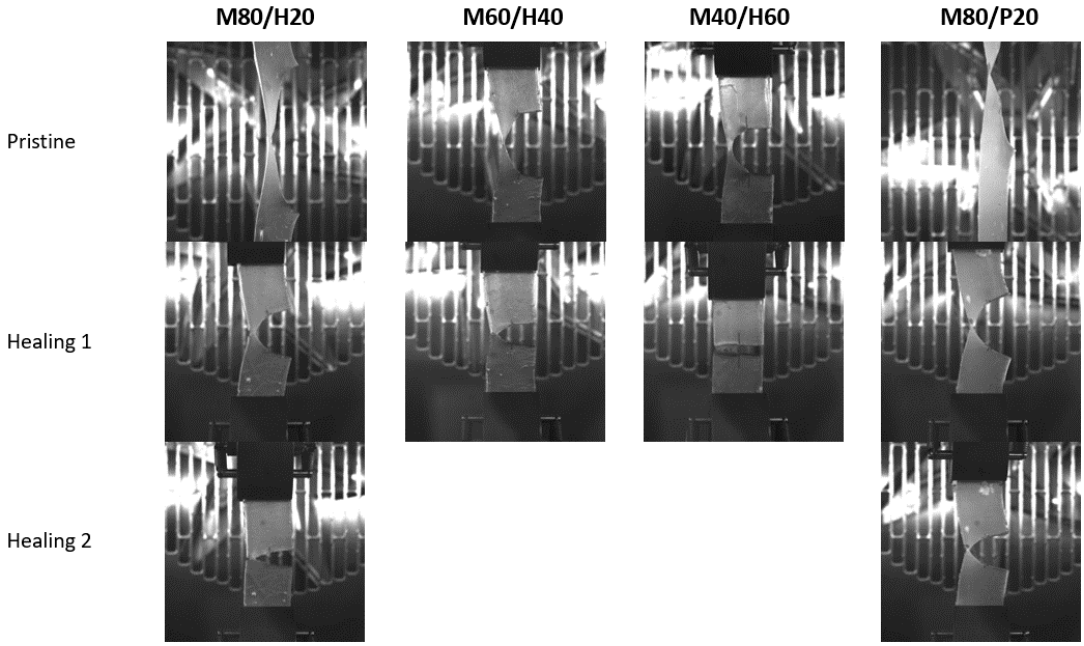

Figure 4.17: Optical images at the moment just before fracture of the pristine and healed samples.

5 IMPACT OF INDUCED AND NATURAL AGEING ON THE MICROSTRUCTURE AND HEALING OF POLYURETHANES

I was taught that the way of progress was neither swift nor easy.

- Marie Skłodowska Curie-

This chapter analyses the effect of temperature and time on the polymer microstructure. On the one hand, the free isocyanate groups detected in the IR spectrum of MDI/HMDI polyurethanes suggest that longer annealing times would be beneficial to promote higher reactivity of these groups to form urethane bonds. On the other hand, the embrittlement observed in the fracture curves of the healed samples M80/H20 and M80/P20 indicates a change of properties over time. Therefore, further testing was required to explain the slow kinetic change observed in these samples.

5.1 Induced ageing: longer annealing times for M80/H20, M60/H40, M40/H60 and M80/P20

The unreacted isocyanate detected in MDI/HMDI random TPU copolymers led to exposing the samples to longer annealing times, as proposed in Reducing the amount of unreacted isocyanate in HMDI-p (appendix). Rather than only observing a reduction in the quantity of unreacted isocyanate, changes in the microstructure were also noticed. Therefore, M80/P20 was also studied in order to conclude whether these changes were exclusively related to the unreacted isocyanate. In this section, the same synthesis procedure was followed with the only alteration that samples were kept for 3 days in the oven instead of 1 day after mixing.

5.1.1 Reduction of unreacted isocyanate

The N=C=O group band is associated to 2275-2270 cm^{-1}. The MDI/HMDI TPUs showed a remarkable peak at 2262 cm^{-1} (Figure 4.1) what is related to certain quantity of unreacted isocyanate. Increasing the quantity of HMDI in the random copolymers clearly led to an increase in the absorbance of N=C=O peaks.

As it is shown in Figure 5.1 and in agreement with the results shown in the appendix (section Reducing the amount of unreacted isocyanate), when the samples are subjected to longer annealing times, the peak associated to N=C=O is reduced. Thus, less unreacted isocyanate is left in the samples when longer annealing times are used. The IR spectrum for 2 days and 3 days was similar, what suggest no further reduction of unreacted isocyanate was achieved after 2 days. For the polymer M80/P20 no changes in the spectra were observed for different annealing times.

In conclusion, annealing times of 2 days or longer facilitate the complete reaction of free isocyanate in MDI/HMDI TPUs.

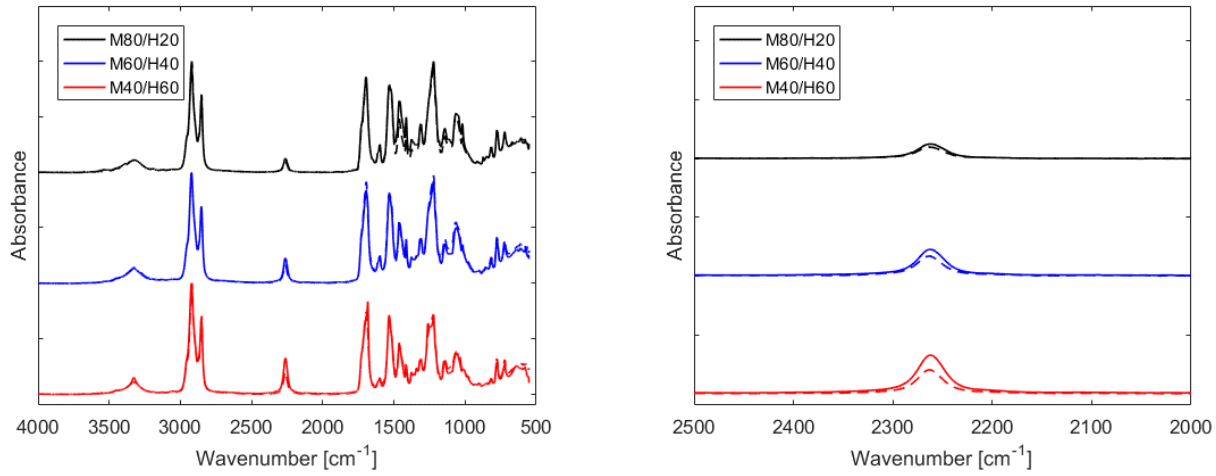

Figure 5.1: FTIR analysis of the MDI/HMDI random TPUs copolymers for different annealing times: 1 day (solid line) and 3 days (dashed line) at 60 ºC.

5.1.2 Microdomains

It can be easily deduced from the results shown in Figure 5.2, that there is a noticeable reduction in the number and dimensions of the micro-domains detected when the annealing time is extended from 1 to 3 days. This effect is stronger for samples with higher content of HMDI, where no clear disperse phase can be detected anymore.

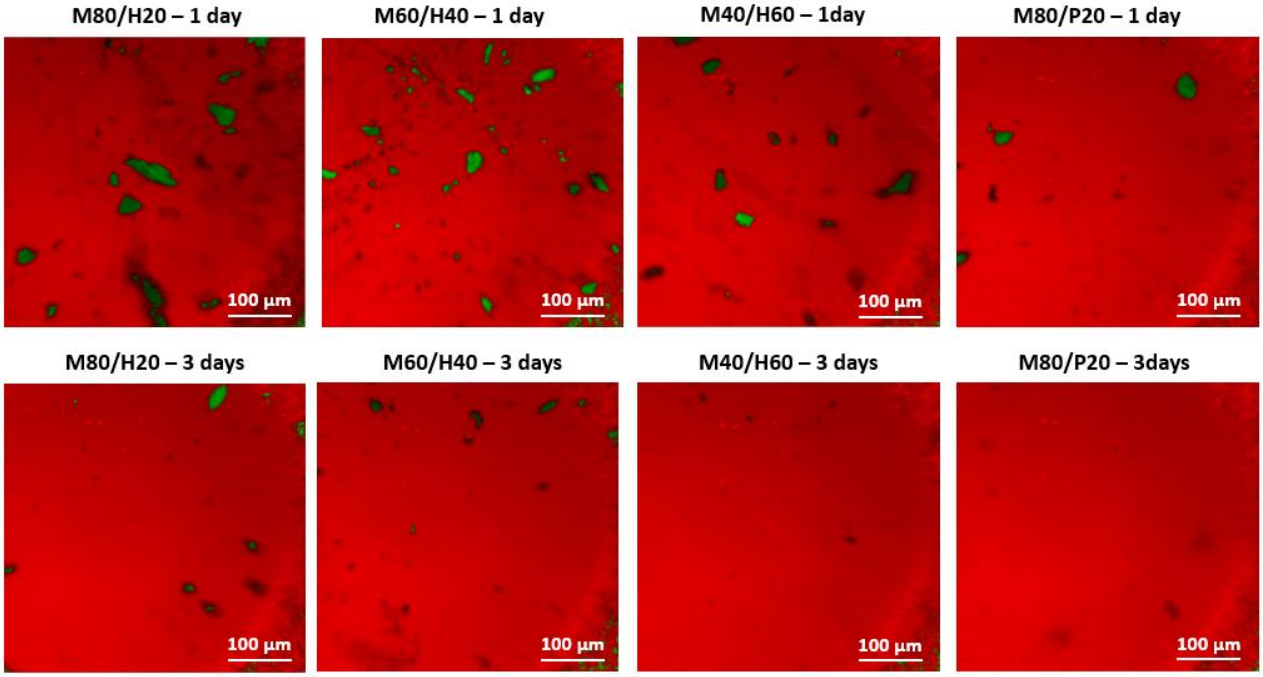

Figure 5.2: FTIR mapping-image for different annealing times (on the surface of the samples).

The decrease in the phase segregation detected can be attributed to a less quantity of unreacted isocyanate originating from HMDI. As previously studied, HMDI-p shows almost no phase segregation (Figure 3.2); therefore, when more HMDI is included in the network, its aliphatic character increases the dispersion, and these hard domains are easily incorporated in the matrix. Nevertheless, this explanation is not applicable for M80/P20 where HMDI is not present and almost no disperse phases are found. Thus, it can be generally assumed that for short annealing times the phases do not have enough time to disperse, while after these 3 days annealing the microdomains increase their solubility in the matrix. The fact that nearly no phase segregation is observed in HMDI-p or M40/H60 can be related to a faster dispersion. Moreover, the results obtained for longer annealing

times agree with C. Prisacariu, who outlines in [11] a greater homogeneity of the polymeric network with annealing time.

While all previous results are always shown for the surface of the polymer, it was necessary to study whether this effect was only a surface or a bulk phenomenon. A thin slab of material was cut in the thicker area of the sample; testing the inner part that was previously in contact with more material. Conducting IR mapping in the bulk of the material, it was concluded that no significant difference could be observed regarding surface/bulk except for M80/H20 where a decrease of disperse phases was found (Figure 5.3).

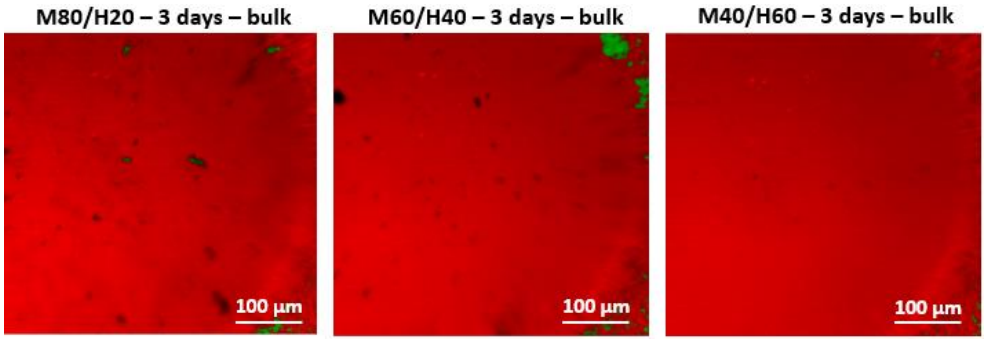

Figure 5.3: FTIR mapping-image of M80/H20, M60/H40 and M40/H20 in the bulk. Annealing time 3 days.

5.1.3 Thermal transitions

As just demonstrated in 5.1.2 Microdomains, when the samples are subjected to longer annealing times, less phase segregation is observed. This can be attributed to a major solubility of the disperse phases into the matrix. In order to demonstrate whether this statement is accurate, DSC tests were conducted in the samples with longer annealing time.

Figure 5.4 collects the results obtained for different annealing times. It should be noted that for the case of M40/H40 the curve for 1 day has been shifted to higher heat flows to facilitate the comparison. When comparing the results for 1 day with the ones for 3 days, three main differences are observed:

1. The endothermic peak detected in the samples annealed for 1 day is larger than the endothermic peak detected in the samples annealed for 3 days. The samples which initially showed more disperse phases (M80/H20 and M80/P20) have considerably reduced the peak more than the others. In the case of M80/P20, no peak is observed.
2. The T_g observed in all the samples annealed for 3 days is slightly higher (Δ~1-3 ºC) than the T_g observed in the samples annealed for 1 day. Thus, although it could indicate that the solubility of the microdomains into the matrix leads to more rigid networks, the variations are very small and, therefore, irrelevant. These results are in agreement with other studies regarding polyamides [43] where no significant changes in the T_g were detected for different annealing times.
3. The endothermic peak still detected in M80/H20, M60/H40 and M40/H60 has been slightly shifted to lower temperature. As for the T_g, these changes are small and, therefore, not relevant.

In conclusion, the fact that less phase segregation and a reduced endothermic peak are observed for the samples subjected to longer annealing times does not provide enough information to support the theory of the hard segments melting. Moreover, this temperature seems to be rather low for the melting of HS. Similar studies with TPUs based on MDI and on HMDI (40 % wt. HS) [39] reported the melting of the HS at temperatures above 170 ºC while the melting due to the crystallization of the SS was detected at 20 ºC. In that same study, they proved that aromatic isocyanates in TPUs hinder the crystallizability of the SS and no peak is detected, as it can be observed for the aromatic based M80/P20. Additionally, the aliphatic character of isocyanates also reduces the tendency to crystallization of SS but in lower degree, being able to observe a peak, as for the case of M80/H20, M60/40 and M40/H60.

In order to shed light on the possible relation between the endothermic peak observed and the crystallization of the SS, the long chain CroHeal™ 2000 was tested. Figure 5.5 displays the results of this test, where a clear endothermic peak at 42.8 ºC can be observed. This temperature is in the same range of the endothermic peaks detected for all the TPUs synthesised (40.5 ºC to 45.5 ºC), what clearly demonstrates the relation between this

melting point and the SS. Moreover, the probable large aliphatic side chains (brushes) present in CroHeal™ 2000 (Figure 2.1) promote the crystallization kinetics, as proved by Vincenzo et al [44] for HDI based TPUs. They also observed that local reactivation of mobility at temperatures below T_{end} was possible for crystallized samples, what supports the significant healing obtained for M80/H20. In [43], Susa et al concluded that the observed melting point (~68 ºC) of the polyimides synthesised was associated to the confinement of the side chains by main chains with lower mobility.

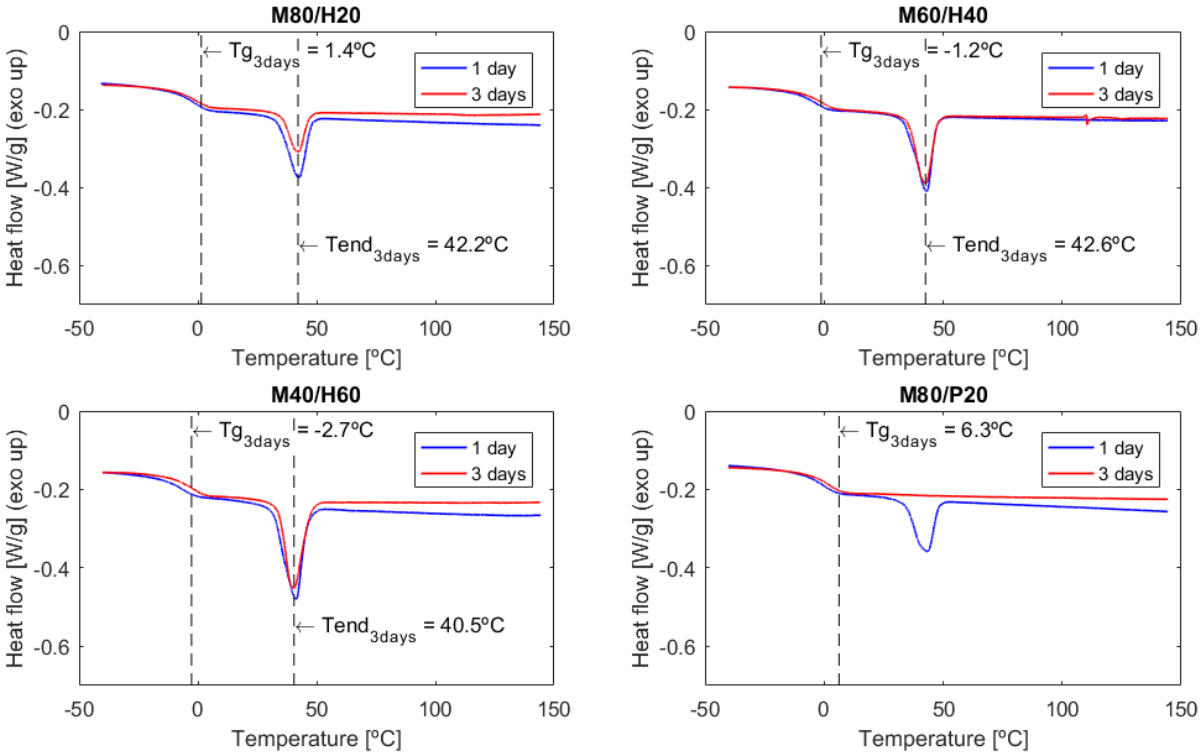

Figure 5.4: DSC first heating curve for different annealing times marking the glass transition temperature (T_g) and the endothermic peak (T_{end}) for the longer annealing time (3 days).

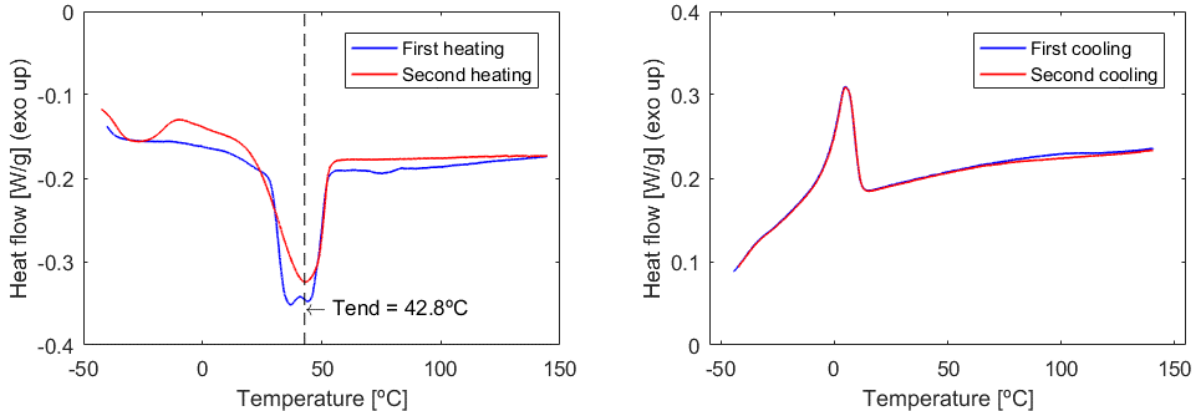

Figure 5.5: DSC first and second heating curves (on the left) and cooling curves (on the right) for CroHeal™ 2000 (component of SS).

5.1.4 Mechanical properties

Figure 5.6 shows how an increase in the duration of the annealing has a direct effect in the mechanical properties. In all cases the toughness and the maximum strength are reduced. M80/H20 and M60/H40 turn into more ductile samples whereas M80/P20 reduces its ductility while keeping almost constant the maximum strength. It was already observed in [18] how different annealing conditions, in that case varying the annealing temperature, lead to significant differences in the mechanical properties of polyurethanes. In [42], different annealing times (1 day, 5 days and 11 days) were used resulting in slightly better mechanical properties except for the case where

crystallization was induced, observed then a significant change.

In 5.1.2, it was shown how less disperse phases were observed after a longer annealing time as a probable result of less incompatibility between hard and soft segments. The presence of less microdomains and, therefore, less concentrated hard segments, could be related to the decrease of the mechanical properties of all samples. The decrease of the mechanical properties could also be attributed to testing the samples too soon after the annealing was completed. Therefore, the change in mechanical properties is not conclusive.

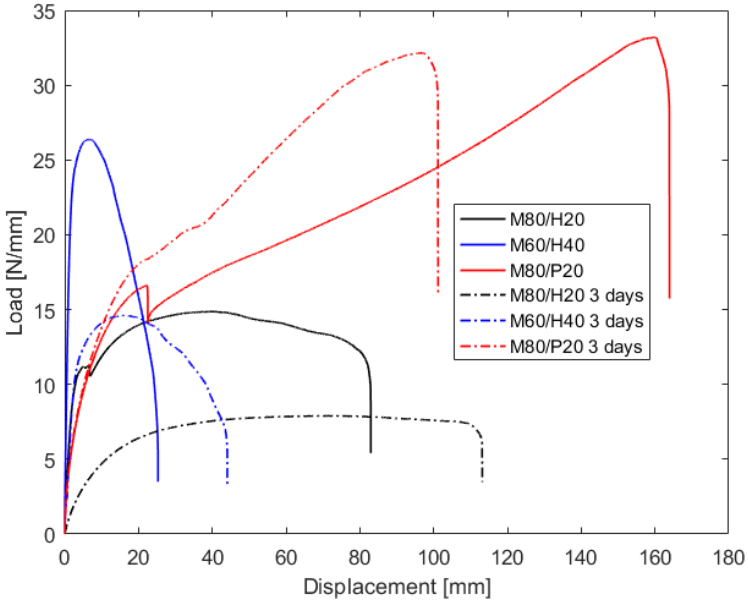

Figure 5.6: Fracture test for the pristine samples for different annealing times.

5.1.5 Healing properties

Fracture tests after healing were performed in longer annealed samples, as shown in Figure 5.7. Unquestionably, lower mechanical properties were obtained for longer annealing times, for both pristine and healed samples. However, the results were not that conclusive for the healing efficiency. As displayed in Figure 5.8, the healing efficiency obtained as the ratio of maximum displacement and the ratio of work done shows nearly no difference for different annealing times. Nevertheless, a larger recovery in the maximum load was detected for M80/H20 and M60/H40 and in the work to failure for M80/H20.

Finally, considering the results presented in 5.1.2, it can be concluded that the disappearance of the microdomains detected with IR mapping does not affect healing.

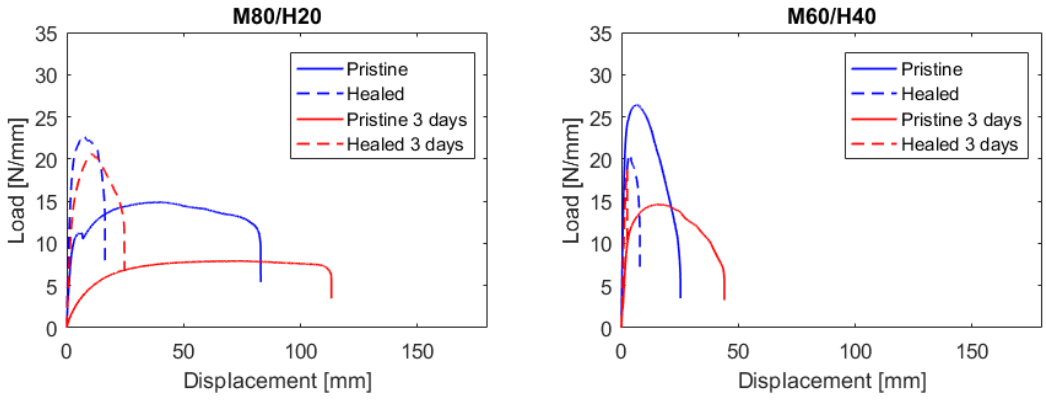

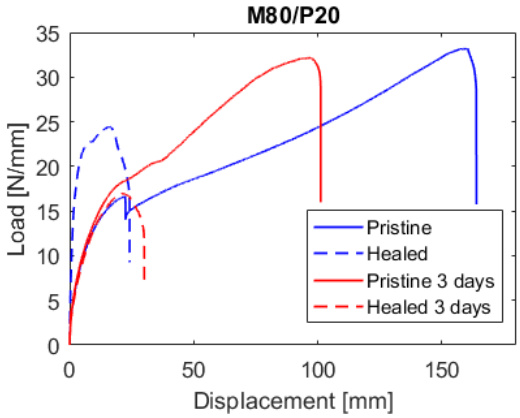

Figure 5.7: Representative load vs. displacement curve of the fracture test of M80/H20, M60/H40 and M60/H20 subjected to longer annealing time.

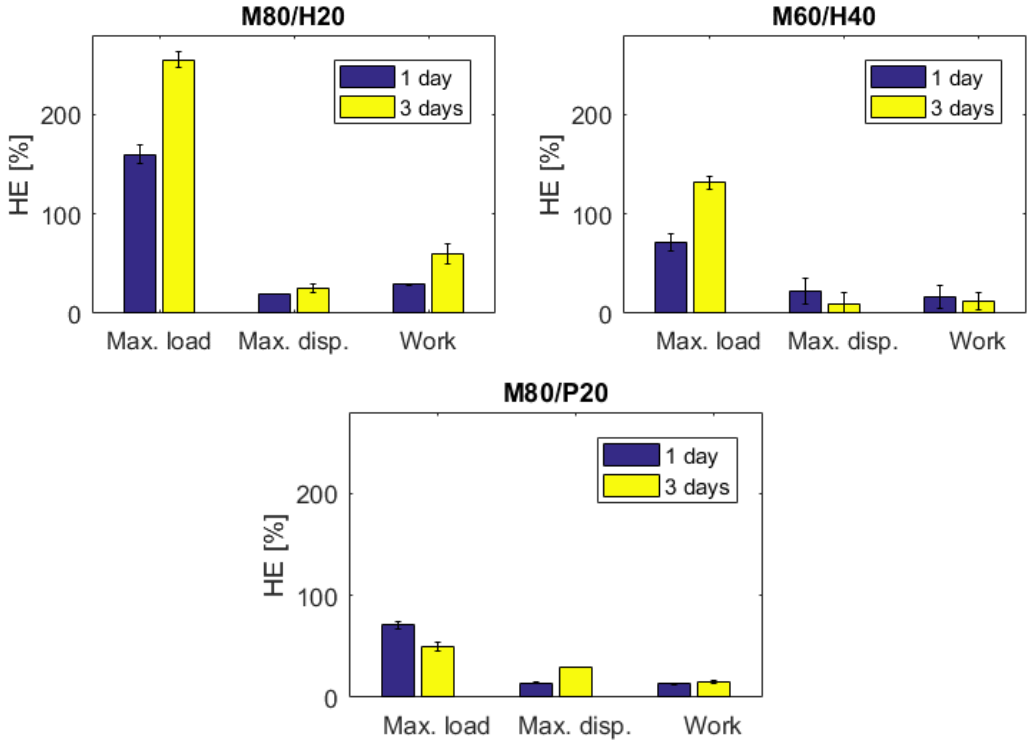

Figure 5.8: Healing efficiency of M80/H20, M60/H40 and M60/H20 subjected to longer annealing times according to maximum load, maximum displacement and work to failure. Error bars are based on two repetitions.

5.2 Natural ageing: embrittlement and strengthening of M80/H20 and M80/P20

The fact that significantly higher strength and/or slope load vs. displacement is obtained for M80/H20 and M80/P20 (Figure 4.14) suggests the existence of an embrittlement process at room temperature. There are different explanations why a polymer can increase its brittleness. In general, the embrittlement of polymers can be associated to chain scission due to exposure to light, heat or oxygen; to the crystallization of the material and to an increase of crosslinks. In this case, the chain scission is not possible as the strength increases. The crystallization is possible as it has already been proved in 5.1.3. Another explanation of this phenomenon is the increase of the physical crosslinks existing in the polyurethane. These hypotheses were investigated via fracture tests, FTIR, FTIR mapping and rheology.

5.2.1 Fracture tests

As the embrittlement was already observed for the healed samples one week after synthesized, it was decided to test the pristine samples aged for 1 month at room temperature to confirm this. Due to the impossibility to synthesize more material and wait for one week, the samples used for the new test were scaled down to ¼ the initial established dimensions (17.5 mm x 5 mm) and cut out of one of the previous original samples. The strain rate applied in the test was also scale down to 0.125 mm/s.

As it can be easily deduced from Figure 5.9, in the case of the samples tested after one month, it can be observed how the healed curve does not surpass the pristine in strength. Therefore, an embrittlement of the material with time is observed.. It should be outlined that even if the mechanical characteristics change, the healing efficiency calculated as the work to failure remains almost the same for the samples as produced and after one month (Table 5.1).

All in all, samples tested as produced led to much more plastic deformation before failure than those stored for one month. This suggests that the former ones did not have enough time after production to homogenise and relax and, therefore, they were tested too early. In conclusion, for future mechanical testing of self-healing polymers samples should only be tested when sufficient time after manufacturing has passed.

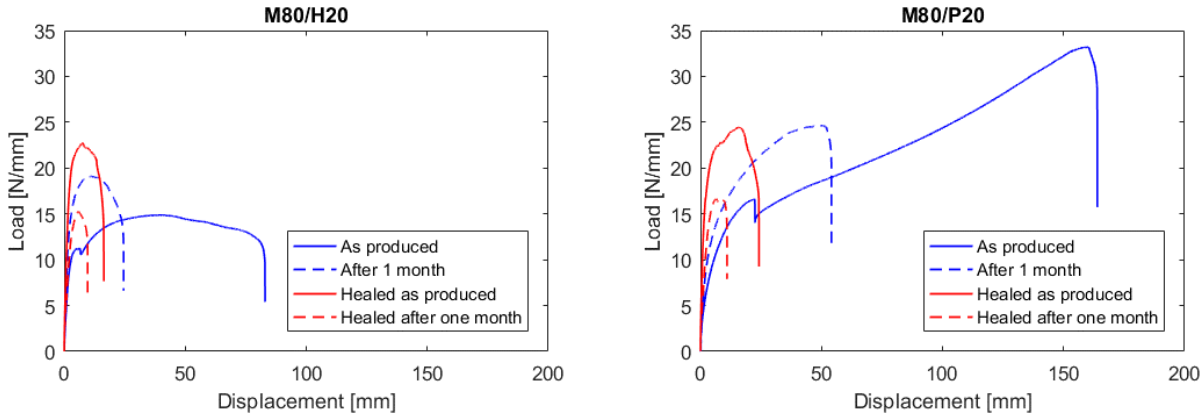

Figure 5.9: Fracture test of pristine samples just synthesized and after 1 month.

Table 5.1: Healing efficiency calculated as the ratio of work to failure for healing conditions 1 week and RT for the samples as produced and after one month.

	HE, as produced [%]	HE, after one month [%]
M80/H20	29	30
M80/P20	13	12

5.2.2 FTIR

The fracture results suggest a change in the properties of the material. Hence, FTIR tests were conducted approximately one month after the synthesis and compared with the results obtained for the samples just synthesized.

As it can be perceived in Figure 5.10 and Figure 5.11, some changes in the spectra were found in the characteristic amide I, amide II, amide III and N-H stretching. In both cases (M80/H20 and M80/P20), two different signals were detected in amide I and amide II bands, in contrast with the sole signal detected in the samples just synthesized, and a sharper peak for N-H was obtained. The broad peak around 3327 cm^{-1} in the samples just synthesized can be associated to the existence of alcohol groups in the molecule. The sharpening of this peak in the samples after one month can be associated to a reduction in the free alcohol that might have reacted with free isocyanate groups leading to more urethane bonds. Therefore, this indicates, as previously speculated, an ageing process.

In the case of M80/H20, the amide I peak has been shifted to lower frequencies, from 1696 cm^{-1} to 1683 cm^{-1}.

However, a shoulder is detected in 1696 cm^{-1}. As already explained in 4.2.2 FTIR, the shift of amide I to lower frequencies is due to H bonds, what supports the theory of higher degree of crosslinking and reaction completion. Moreover, stronger peaks are observed for amide I and amide II, both related to the H bonds in soft segments and hard segments. A new peak is also observed very close to the amide III band, in 1261 cm^{-1}, which can be attributed to the group -C(=O)-O-C- present in the polyol. In relation to the spectra of M80/P20, a double peak in the amide I band is found, in 1695 cm^{-1} and 1684 cm^{-1}. Moreover, a smooth shoulder is found close to amide III band and stronger absorption for amide II is obtained. The stronger absorption is, as for M80/H20, related to more H bonds presents.

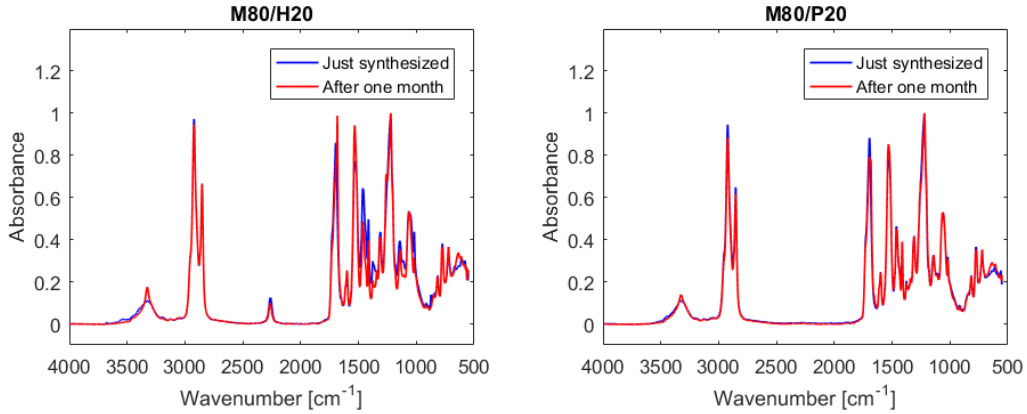

Figure 5.10: FTIR analysis for different moments after synthesis of M80/H20 and M80/P20.

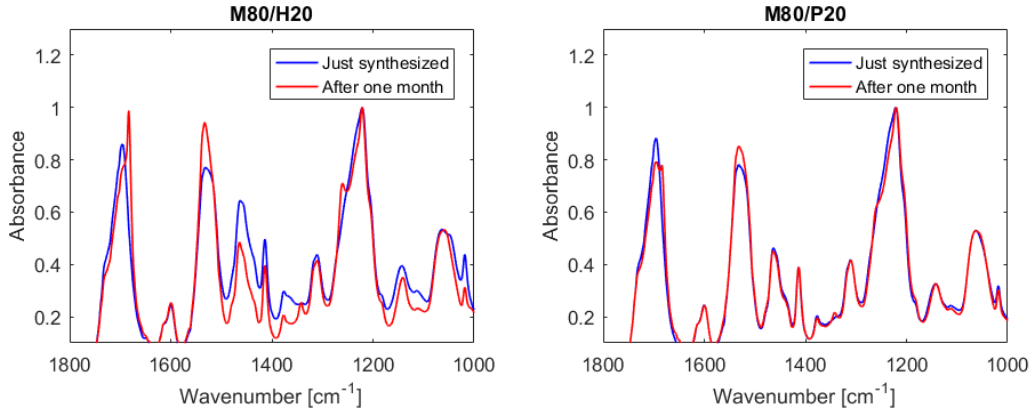

Figure 5.11: Magnified view of FTIR analysis for different moments after synthesis of M80/H20 and M80/P20.

5.2.3 Microdomains

For the sample M80/H20, a small decrease over time on the percentage of microdomains detected with the FTIR mapping was observed, as also obtained for longer annealing times (Figure 5.2). These results suggest that a more homogeneous distribution of the hard segments in the matrix can lead to an increase in the strength of the overall network as long as sufficient time is left for the samples to homogenise and relax after production.

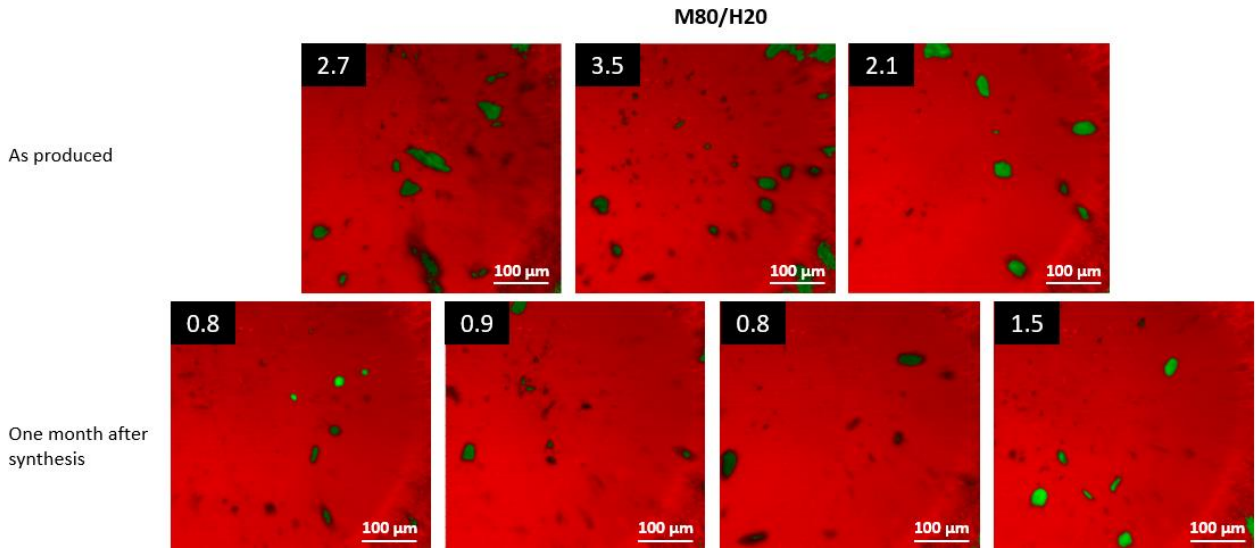

Figure 5.12: FTIR mapping-images of M80/H20 as produced and one month after synthesis. The percentage of disperse phase of each image is included in the top left corner.

5.2.4 Rheology

Another temperature sweep test (Figure 5.13) was conducted for the polymer M80/H20 after roughly one month starting from the glassy region (-10 ºC) until the rubbery region in order to compare the results regarding the T_g with the ones obtained from the DSC and to analyse possible changes in the crossover temperature.

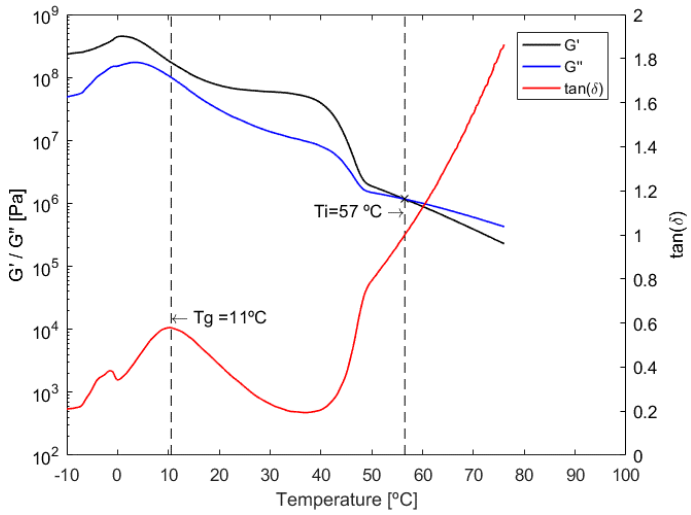

Figure 5.13: Temperature sweep rheology for M80/H20 starting from -10 ºC.

As displayed in Figure 5.13, the dynamic shear storage modulus (G') starts decreasing at 1 ºC and the relaxation peak from the mechanical glass transition temperature of soft segments is detected at 11 ºC when the damping factor or tan(δ) (i.e. ratio of energy lost per energy stored (G''/G')) is maximum. The mechanical T_g is higher than the thermal T_g determined by DSC (-0.4 ºC), which can be attributed to intrinsic differences between these two different techniques. Tan(δ) shows a stepwise glass transition (already reported in literature [43]) that can be attributed to the copolymeric nature of the polymers. The rubbery plateau region starting from 11 ºC is extended until 40 ºC where a sharp decrease in G' is experienced. From 40 ºC, the material starts flowing, having its crossover around 57 ºC. Thus, an increase in the crossover is also detected for the rheology test compared with the results analysed in Figure 4.12 (conducted within less than one week after the synthesis). If more H bonds are formed with time, then the flexibility of the network would decrease and higher crossover would be expected, as confirmed by Figure 5.13.

It is also interesting to highlight how the sharp decrease in G' is experienced at 40 ºC, very similar to the endothermic peak detected in the DSC. This clearly indicates that the peak obtained in the DSC is a melting peak.

In conclusion the embrittlement can be related to an increase in the H bonds formed (reaction completion), clearly supported by the FTIR results, but also to the crystallization of the SS. To prove this last hypothesis, DSC tests should be conducted for the samples as produced in order to compare with the ones already presented in Figure 4.6 which already show crystallization of the SS and were conducted 1 week after the samples were synthesized.

6 CONCLUSIONS AND RECOMMENDATIONS

Winning the prize wasn't half as exciting as doing the work itself.

- Maria Goeppert-Mayer -

The results presented in the previous chapter analyse the characteristics and potential healing of nine different TPUs. From all the testing procedures and results obtained some conclusions and future recommendations should be exposed.

6.1 Conclusions

The use of different isocyanates to produce TPUs was investigated. TPUs with a mixture of different isocyanates clearly showed potential as a self-healing material. The main conclusions that can be drawn from this research project are:

- The synthesis of TPUs based on PPDI was rather complicated due to the tendency of PPDI to from crystals before melting and its rapid solidification when poured into the mixture of polyols.
- Unreacted isocyanate was detected in the FTIR spectrum of the matrix of HMDI-p and MDI/HMDI TPUs. The peak associated to the free isocyanate reduced with longer times at 60 ºC to complete the reaction.
- Micro-phase segregation attributed to a larger content of hard domains was detected with IR mapping. The presence of H bonds promoting healing was demonstrated. The percentage of phase segregation decreases as follows: MDI > PPDI > HMDI. For MDI/HMDI TPUs, as HMDI increases, the phase segregation decreases. For MDI/PPDI TPUs no clear tendency is found.
- A significant decrease in the crossover in rheological studies for polymers combining MDI and HMDI was observed, suggesting higher mobility of the polymeric network at lower temperatures. This demonstrates the dominance of the aliphatic diisocyanate providing more flexibility.
- The highest healing efficiency are obtained for M80/H20 and M80/P20, being the only ones able to heal twice. The flexibility provided by the 20 % of HMDI results advantageous when compared with MDI-p.
- Longer annealing times contribute to the disappearance of the microdomains detected with IR mapping. The samples subjected to longer annealing times showed no clear difference in healing. This suggests that the microdomains do not affect healing.
- Crystallization of the side branches in the SS is observed for all polymers based on mixtures of diisocyanates. This crystallization is slightly reduced with annealing. For the case of mixtures of aromatics, no crystallization is observed after annealing.

- The embrittlement observed in the fracture curves of the healed samples was demonstrated to be related to an increase of the degree of physical crosslinking.
- The larger plastic deformation of the samples as produced and the samples subjected to longer annealing times in comparison with the samples after one month outlines the importance of sufficient resting time between manufacturing and testing.

To summarize, M80/H20 and M80/P20 are the two random copolymers which have provided the most promising results concerning healing at room temperature, being able to considerably recover their mechanical properties even after second healing. On the one hand, although the mechanical properties and second healing efficiency were higher for M80/P20, the use of PPDI entails a more difficult synthesis. Moreover, M80/H20 considerably increased its mobility in comparison to MDI-p, showing the largest first healing efficiency at room temperature. However, its properties significantly change with time, suffering embrittlement.

Longer annealing times help homogenizing the polymers with lower presence of microdomains and more complete reactions. Fracture tests revealed that no remarkable changes in the healing efficiency are experienced. Therefore, the larger healing efficiency obtained for MDI-p, PPDI-p, M80/H20 and M80/P20 is associated with the aromatic character of the hard segments rather than to the disperse phases observed.

6.2 Recommendations

The work done for this project can be extended and improved following some recommendations:

- The miscibility issues faced with PPDI can be improved using a two-step synthesis procedure.
- A minimum resting time of one week between manufacturing and testing is needed is recommended.
- Scanning electron microscope and confocal scanning laser microscope can provide additional information about the healing mechanisms as a function of the surface roughness [5].
- Healing at higher temperatures (e.g. 60 ºC) can provide further information about the interphase healing response.
- Synthesis of polyol and diisocyanates and synthesis of chain extender and diisocyanates may further elucidate the role of SS and HS.
- Frequency sweep tests are recommended in order to understand the dominance of the viscous or elastic behaviour at the selected shear rate applied for the fracture tests and the relaxation behaviour of these TPUs.
- The use of at least three samples per polymer and synthesis and healing conditions is highly recommended to provide more accurate results.
- The use of certain manufacturing techniques such as injection moulding could help achieving a more constant thickness for the fracture test samples.
- The research into alternatives to assess more efficiently the phase segregation is recommended. In this project, more than 50 FTIR mapping tests were conducted, what translated into more than 34 hours testing and changing sample every 41 minutes. Furthermore, the difficulty of achieving a good enough contact between crystal and sample led to the failure of several tests.
- The printability already shown by MDI-p in previous works [45], suggests the polymers synthesized can be a good asset for FDM applications. Therefore, further study is required following the recommendations already stated in [45].

REFERENCES

[1] S. Van Der Zwaag, "Self-Healing Materials: An Alternative Approach to 20 Centuries of Materials Science," *Chem. Int. -- Newsmag. IUPAC*, 2014.

[2] M. D. Hager, P. Greil, C. Leyens, S. Van Der Zwaag, and U. S. Schubert, "Self-healing materials," *Adv. Mater.*, 2010.

[3] Y. M. Malinskii, V. V. Prokopenko, N. A. Ivanova, and V. A. Kargin, "Investigation of self-healing of cracks in polymers," *Polym. Mech.*, 1973.

[4] S. C. G. Leeuwenburgh, N. De Belie, and S. van der Zwaag, "Self-Healing Materials are Coming of Age," *Advanced Materials Interfaces*. 2018.

[5] A. M. Grande, S. J. Garcia, and S. Van Der Zwaag, "On the interfacial healing of a supramolecular elastomer," *Polymer (Guildf).*, 2015.

[6] S. J. Garcia, "Effect of polymer architecture on the intrinsic self-healing character of polymers," *European Polymer Journal*. 2014.

[7] Y. Yang and M. W. Urban, "Self-healing polymeric materials," *Chem. Soc. Rev.*, 2013.

[8] C. Kim and N. Yoshie, "Polymers healed autonomously and with the assistance of ubiquitous stimuli: how can we combine mechanical strength and a healing ability in polymers?," *Polymer Journal*. 2018.

[9] J. -M Lehn, "Supramolecular Chemistry—Scope and Perspectives Molecules, Supermolecules, and Molecular Devices (Nobel Lecture)," *Angew. Chemie Int. Ed. English*, 1988.

[10] Y. Yang, X. Ding, and M. W. Urban, "Chemical and physical aspects of self-healing materials," *Progress in Polymer Science*. 2015.

[11] C. Prisacariu, "Polyurethane Elastomers : From Morphology to Mechanical Aspects," *Polyurethane Elastomers From Morphol. to Mech. Asp.*, 2011.

[12] M. S. Sánchez-Adsuar, "Influence of the composition on the crystallinity and adhesion properties of thermoplastic polyurethane elastomers," *Int. J. Adhes. Adhes.*, 2000.

[13] H. Do Kim, J. H. Huh, E. Y. Kim, and C. C. Park, "Comparison of properties of thermoplastic polyurethane elastomers with two different soft segments," *J. Appl. Polym. Sci.*, 1998.

[14] I. Javni *et al.*, "Thermoplastic polyurethanes with controlled morphology based on methylenediphenyldiisocyanate/isosorbide/butanediol hard segments," *Polym. Int.*, 2015.

[15] Private communication (1) - Research conducted at NovAM, 2019.

[16] I. Yilgor, E. Yilgor, I. G. Guler, T. C. Ward, and G. L. Wilkes, "FTIR investigation of the influence of diisocyanate symmetry on the morphology development in model segmented polyurethanes," *Polymer (Guildf).*, 2006.

[17] C. Prisacariu, E. Scortanu, I. Stoica, B. Agapie, and V. Barboiu, "Morphological features and thermal and mechanical response in segmented polyurethane elastomers based on mixtures of isocyanates," *Polym. J.*, 2011.

[18] C. Prisacariu, R. H. Olley, A. A. Caraculacu, D. C. Bassett, and C. Martin, "The effect of hard segment ordering in copolyurethane elastomers obtained by using simultaneously two types of diisocyanates," *Polymer (Guildf).*, 2003.

[19] J. P. Sheth, D. B. Klinedinst, G. L. Wilkes, I. Yilgor, and E. Yilgor, "Role of chain symmetry and hydrogen bonding in segmented copolymers with monodisperse hard segments," *Polymer (Guildf).*,

2005.

[20] H. Ulrich, *Chemistry and Technology of Isocyanates*. New York: John Wiley and Sons, 1996.

[21] R. Bhargava, S. Q. Wang, and J. L. Koenig, "FTIR microspectroscopy of polymeric systems," *Advances in Polymer Science*. 2003.

[22] C. Prisacariu and I. Agherghinei, "Reactions in solid state within polyurethanes. Kinetics and postcure reaction mechanism in casting polyurethane elastomers," *J. Macromol. Sci. - Pure Appl. Chem.*, 2000.

[23] D. Klempner and K. C. Frisch, *Advances in urethane science and technology*, Shrewsbury. Rapra Technology, 1981.

[24] T. J. Touchet and E. M. Cosgriff-Hernandez, "Hierarchal Structure-Property Relationships of Segmented Polyurethanes," in *Advances in Polyurethane Biomaterials*, 2016.

[25] J. W. C. Van Bogart, P. E. Gibson, and S. L. Cooper, "Structure-property relationships in polycaprolactone-polyurethanes.," *J. Polym. Sci. Part A-2, Polym. Phys.*, 1983.

[26] S. Burattini *et al.*, "A healable supramolecular polymer blend based on aromatic π-π Stacking and hydrogen-bonding interactions," *J. Am. Chem. Soc.*, 2010.

[27] C. Zhang, Z. Ren, Z. Yin, H. Qian, and D. Ma, "Amide II and amide III bands in polyurethane model soft and hard segments," *Polym. Bull.*, 2008.

[28] H. S. Lee, Y. K. Wang, and S. L. Hsu, "Spectroscopic Analysis of Phase Separation Behavior of Model Polyurethanes," *Macromolecules*, 1987.

[29] V. L. Furer, "The IR spectra and hydrogen bonding of toluene-2,6-bis(methyl) and 4,4'-diphenylmethane-bis(methyl) carbamates," *J. Mol. Struct.*, 2000.

[30] L. Jiang, Z. Ren, W. Zhao, W. Liu, H. Liu, and C. Zhu, "Synthesis and structure/properties characterizations of four polyurethane model hard segments," *R. Soc. Open Sci.*, 2018.

[31] V. W. Srichatrapimuk and S. L. Cooper, "Infrared Thermal Analysis Of Polyurethane Block Polymers," *J. Macromol. Sci. Part B*, 1978.

[32] F. Chen and Z. Lu, "Liquefaction of wheat straw and preparation of rigid polyurethane foam from the liquefaction products," *J. Appl. Polym. Sci.*, 2009.

[33] Z. S. Petrović, Z. Zavargo, J. H. Flyn, and W. J. Macknight, "Thermal degradation of segmented polyurethanes," *J. Appl. Polym. Sci.*, 1994.

[34] A. A. Abdel Hakim, M. Nassar, A. Emam, and M. Sultan, "Preparation and characterization of rigid polyurethane foam prepared from sugar-cane bagasse polyol," *Mater. Chem. Phys.*, 2011.

[35] R. H. Krämer, M. Zammarano, G. T. Linteris, U. W. Gedde, and J. W. Gilman, "Heat release and structural collapse of flexible polyurethane foam," *Polym. Degrad. Stab.*, 2010.

[36] J. M. Cervantes-Uc *et al.*, "TGA/FTIR studies of segmented aliphatic polyurethanes and their nanocomposites prepared with commercial montmorillonites," *Polym. Degrad. Stab.*, 2009.

[37] Y. Camberlin and J. P. Pascault, "Quantitative dsc evaluation of phase segregation rate in linear segmented polyurethanes and polyurethaneureas.," *J. Polym. Sci. A1.*, 1983.

[38] Y. Camberlin and J. P. Pascault, "Phase segregation kinetics in segmented linear polyurethanes: relations between equilibrium time and chain mobility and between equilibrium degree of segregation and interaction parameter.," *J. Polym. Sci. Part A-2, Polym. Phys.*, 1984.

[39] D. K. Lee and H. B. Tsai, "Properties of segmented polyurethanes derived from different diisocyanates," *J. Appl. Polym. Sci.*, 2000.

[40] C. H. Y. Chen, R. M. Briber, E. L. Thomas, M. Xu, and W. J. MacKnight, "Structure and morphology of segmented polyurethanes: 2. Influence of reactant incompatibility," *Polymer (Guildf).*, 1983.

[41] T. K. Kwei, "Phase separation in segmented polyurethanes," *J. Appl. Polym. Sci.*, 1982.

[42] A. Susa, A. Mordvinkin, K. Saalwächter, S. Van Der Zwaag, and S. J. Garcia, "Identifying the Role of Primary and Secondary Interactions on the Mechanical Properties and Healing of Densely Branched Polyimides," *Macromolecules*, 2018.

[43] A. Susa, J. Bijleveld, M. Hernandez Santana, and S. J. Garcia, "Understanding the Effect of the Dianhydride Structure on the Properties of Semiaromatic Polyimides Containing a Biobased Fatty Diamine," *ACS Sustain. Chem. Eng.*, 2018.

[44] V. Montano, M. M. B. Wempe, S. M. H. Does, J. C. Bijleveld, S. Van Der Zwaag, and S. J. Garcia, "Controlling Healing and Toughness in Polyurethanes by Branch-Mediated Tube Dilation," *Macromolecules*, 2019.

[45] Private communication (2) - Research conducted at NovAM, 2020.

[46] K. C. Cole, P. Van Gheluwe, M. J. Hébrard, and J. Leroux, "Flexible polyurethane foam. I. FTIR analysis of residual isocyanate," *J. Appl. Polym. Sci.*, 1987.

[47] G. G. Greth, R. G. Smith, and G. O. Rudkin, "The Determination and Effect of Unreacted Isocyanate Groups in Rigid Urethane Foams," *J. Cell. Plast.*, 1965.

[48] I. S. Ristić *et al.*, "The properties of polyurethane hybrid materials based on castor oil," *Mater. Chem. Phys.*, 2012.

[49] S. Luo, H. Tan, J. Zhang, Y. Wu, F. Pei, and X. Meng, "Catalytic mechanisms of triphenyl bismuth, dibutyltin dilaurate, and their combination in polyurethane-forming reaction," *J. Appl. Polym. Sci.*, 1997.

APPENDIX

Reducing the amount of unreacted isocyanate in HMDI-p

HMDI-p showed considerably lower mechanical properties (see 3.2.5 Fracture tests of pristine samples) and less healing efficiency (see 3.2.6 Healing characterization) than other polyurethanes such as MDI-p and PPDI-p. This can be related to incomplete reaction of the isocyanate found in FTIR measurements (Figure 3.1). The unreacted isocyanate outlines a lack of formation of urethane groups, key for the hard segments and, therefore, for the overall properties of the material. Hereby, different ways to reduce the amount of unreacted isocyanate were explored modifying the synthesis procedure for HMDI-p described 3.1 Polymer synthesis.

As found in literature [46][47], unreacted isocyanate has also been reported in previous researches with toluene diisocyanate (TDI) even when less than the stochiometric amount of diisocyanate was used. On the other hand, other studies which synthesised castor oil and TDI showed that when no excess of isocyanate was used, the absorbance for these groups was zero [48].

As the reaction kinetics associated to HMDI are slower than with respect to other isocyanates [11], it was suggested that longer times at 60 ºC were needed in order to complete the reaction. Therefore, the same sample was tested after 1 day (already shown in Figure 3.1), 2 days and 5 days kept in the oven after synthesis.

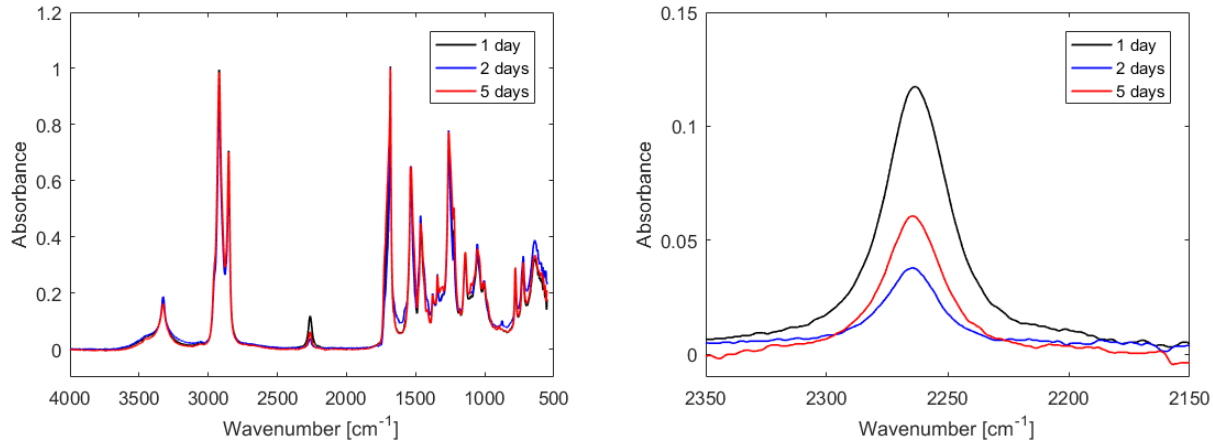

Figure A.1: FTIR analysis of HMDI-p for different times in the oven (1 day, 2 days and 5 days) at a temperature of 60 ºC. The right plot shows a magnified view of the isocyanate peak.

Figure A.1 clearly shows a reduction in the quantity of unreacted isocyanate when the sample is kept for longer times in the oven, with a significant drop between 1 and 2 days. The spectra for 2 days and 5 days in less conclusive, attributed to the variability of the area tested, and advocates no significant difference in the quantity of free isocyanate.

As longer times did not lead to the full disappearance of unreacted isocyanates, it was decided to increase the mixing time in the SpeedMixer to achieve a more homogeneous material able to react more easily. It should be noticed that when less quantity of material was synthesized (10 g of polyol instead of 30 g), the material obtained was not homogeneous with clear miscibility problems were observed between the polyol, the diol and isocyanate. This indicates the necessity to adjust the mixing parameters according to the quantity produced.

The new mixing times were 120 seconds to achieve vacuum, instead of the previous 15 seconds, and 180 seconds at 2300 rpm instead of 160 seconds. The longer vacuum time had the target of achieving a totally bubble free sample, although generally this was not a problem. The longer mixing aimed at increasing the homogeneity of the sample during the mixing. Figure A.2 exhibits that a longer mixing time led to a small reduction unreacted

isocyanate after 2 days in the oven. It should be noted that, contrary to what was expected, the FTIR after 1 day in the oven showed higher isocyanate for the sample mixed for longer times.

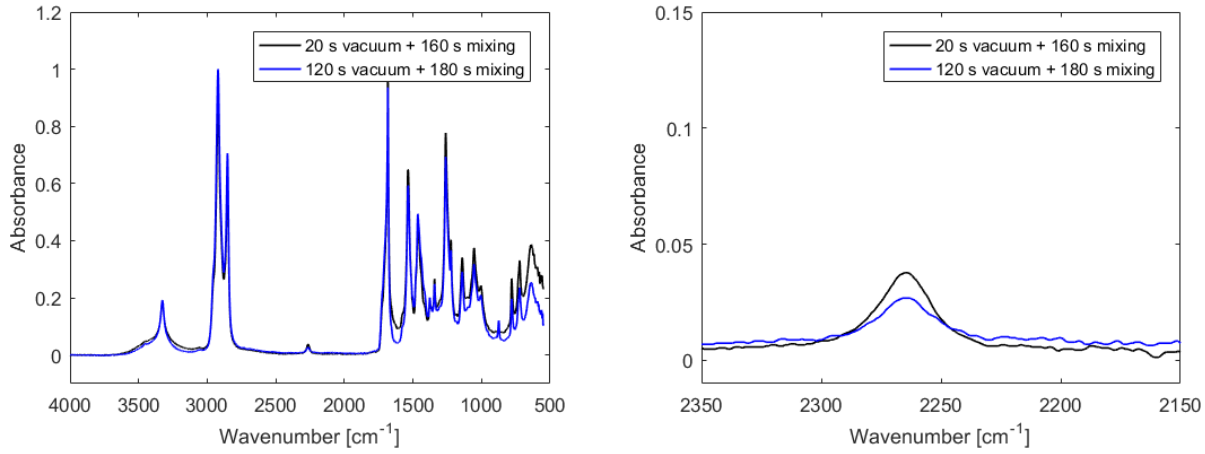

Figure A.2: FTIR analysis of HMDI-p for different mixing times (160 s and 180 s). On the right, complete spectra and, on the left, peak of unreacted isocyanate. Both samples were 2 days in the oven at 60 ºC.

In order to evaluate if the unreacted isocyanate was due to the initial excess of isocyanate (10 %), a new synthesis with no excess isocyanate was prepared, thereby modifying the molar ratio between the reactants for the polymer synthesis. The sample was kept in the oven for 2 days. As it can be observed in the Figure A.3, no appreciable changes were perceived in the unreacted isocyanate peak when using 0% or 10% excess.

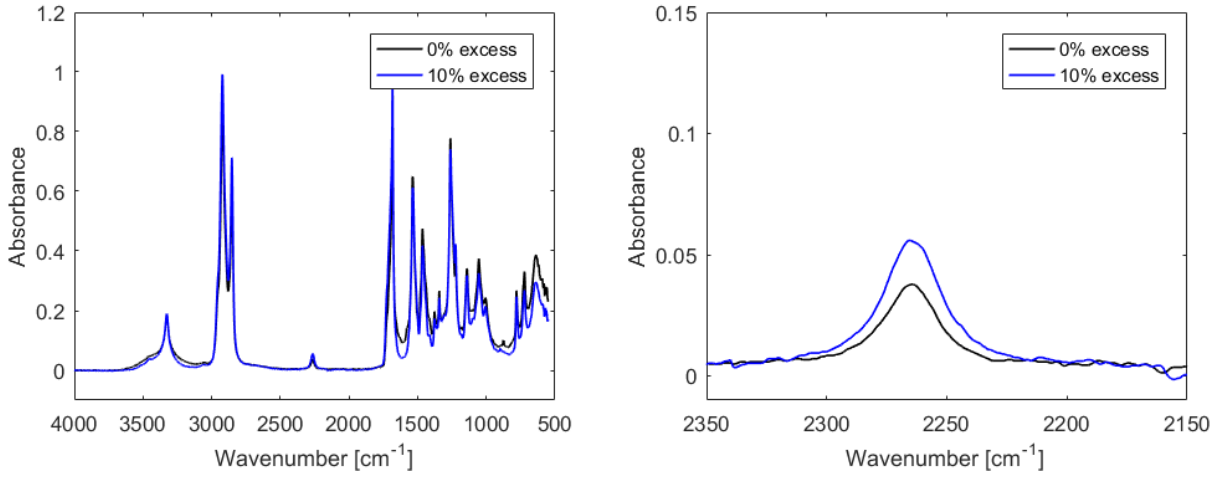

Figure A.3: FTIR analysis of HMDI-p for N=C=O/OH ratios (1.1 and 1). On the right, complete spectra and, on the left, peak of unreacted isocyanate. Both samples were 2 days in the oven at 60 ºC.

Based on the previous tests it was concluded that the cause of the unreacted isocyanate was probably due to the lower reactivity of the HMDI. For this reason, one last synthesis was conducted using a catalyst. For this purpose, 5 droplets (approximately 0.25 mL and 0.8 % weight) of DBTL were added to the composition using 10 % excess of isocyanate and letting react for 2 days in the oven. Figure A.4 shows the comparison between this catalysed sample after 1 day in the oven and the non-catalysed one after 2 days.

The results unquestionably demonstrate that a complete reaction of the isocyanate is achieved using the catalyst even if the sample is only kept in the oven for 1 day (Figure A.4). Nevertheless, when handling the material a clear alteration of its mechanical properties was noticed. While the material without catalyst presented normal elastomeric properties such as easy to deform and flexibility, the polymer with DBTDL was highly brittle. This material alterations have already been stated in literature: the use of catalysts for the formation of the urethane linkages is not easy due to the fact that this type of reactions are subjected to various side reactions besides the fact that the selected catalyst and quantity used can considerably alter the properties of the polymer obtained [49]. Therefore, the brittleness of the resultant polymer can be due to an excessive quantity of catalyst.

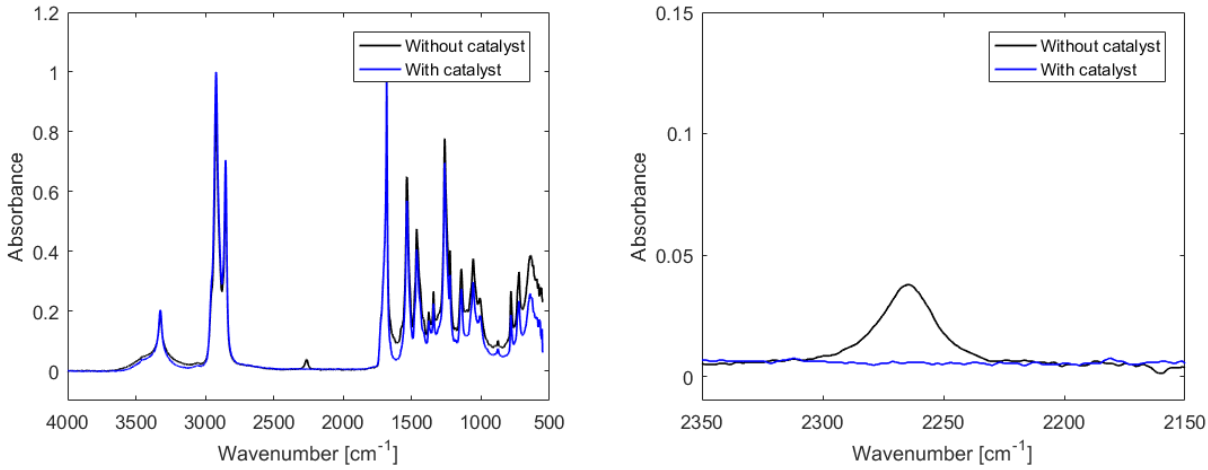

Figure A.4: FTIR analysis of HMDI-p with DBTDL as a catalyst (1 day in the oven) and without catalyst (2 days in the oven). On the right, complete spectra and, on the left, peak of unreacted isocyanate.

In conclusion, considering the results presented, the easiest way to achieve an almost unreacted isocyanate free sample without altering the mechanical properties is to keep the polymer in the oven for at least 2 days. The use of catalyst also shows promising advantages, but further tests should be done adding less quantity of DBTDL or a different catalyst.

No further study than FTIR measurements was performed with the samples of HMDI-p kept for 2 days in the oven and, therefore, no conclusion regarding the effect on healing or mechanical properties was obtained.

FTIR mapping

At least three FTIR mapping measurements were conducted for each type of TPU. The percentage of disperse phases detected in each image is shown on a black square on the top left corner. For each polymer, the average percentage of disperse phases and the standard deviation of these values is included. These values coincide with the ones already shown in Table 3.3 and Table 4.5.

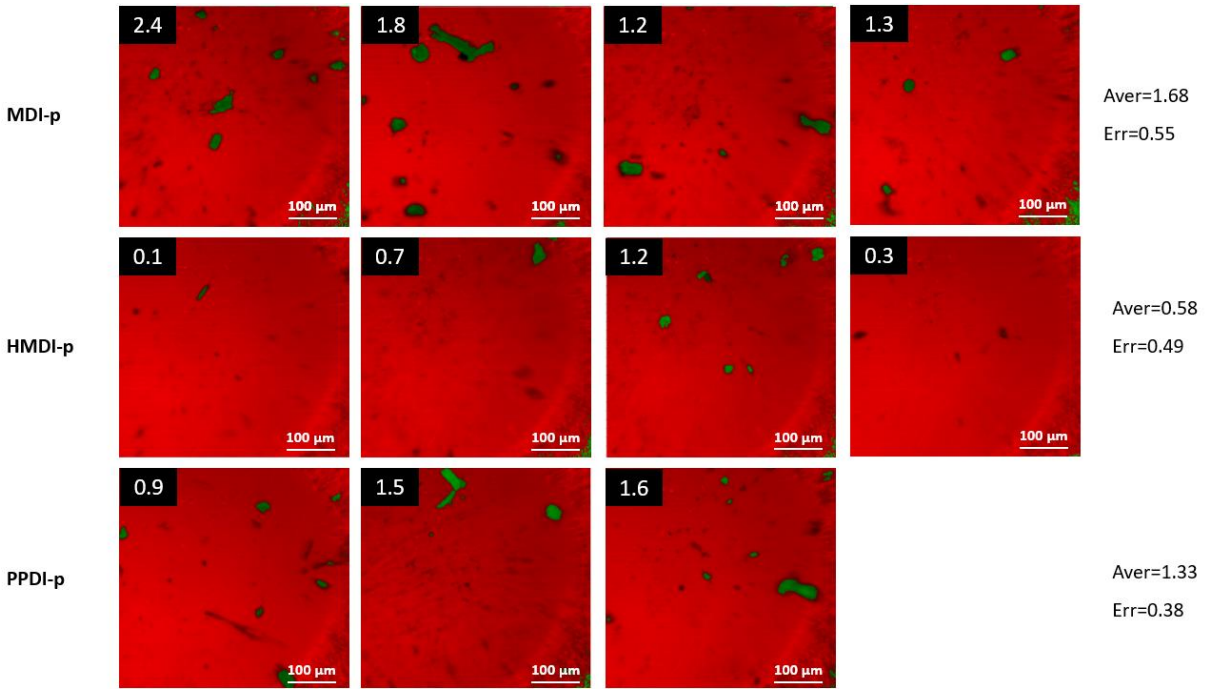

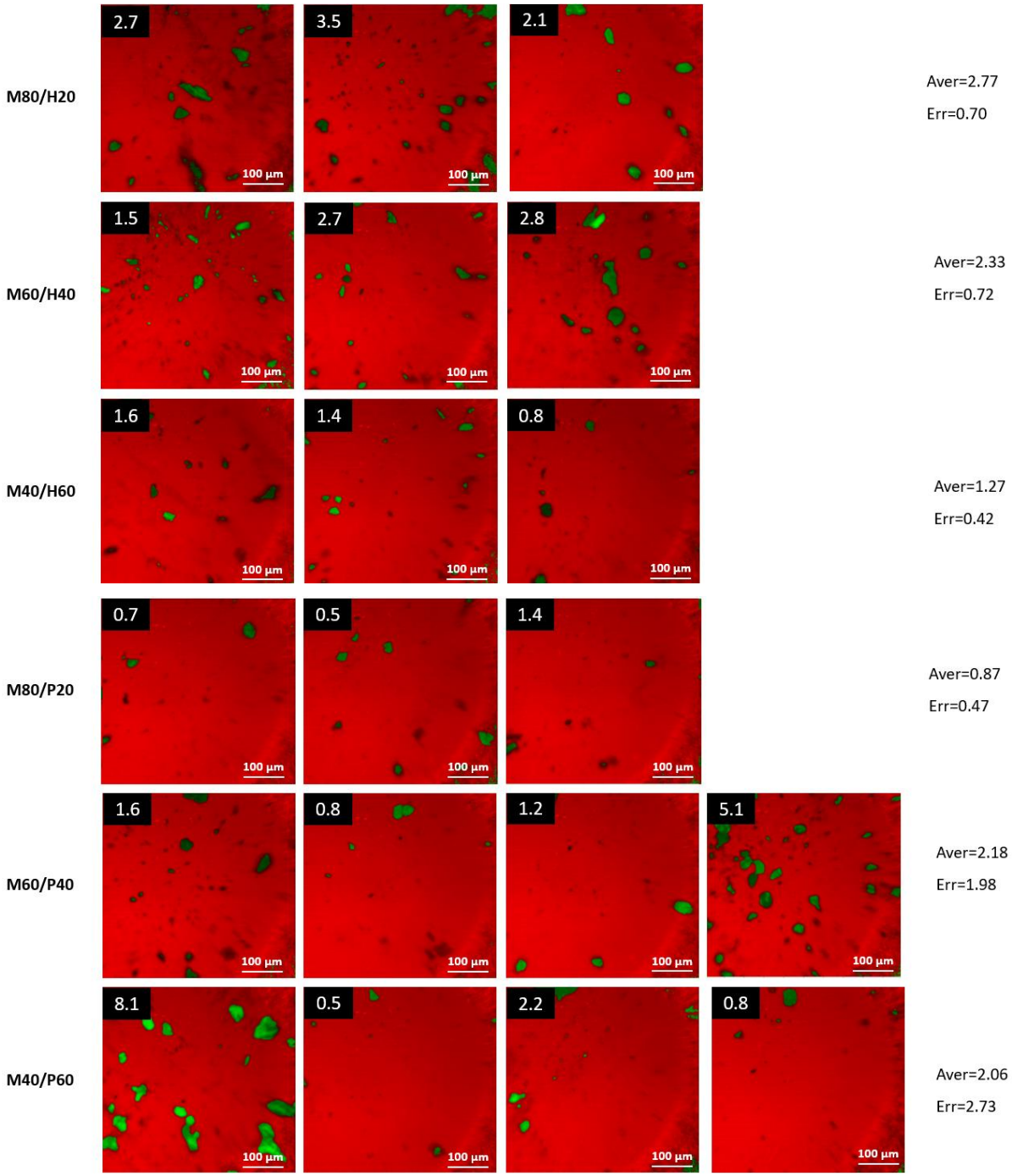

Figure A.5: FTIR mapping-image of all the polyurethanes synthesized. In the right side, the average (aver) and the standard deviation (err) is included.

Fracture test

All samples previously tested were healed at room temperature for one week. In order to explore the impact on healing of applying healing temperatures above the crossover of the sample, one sample of M80/H20 was placed in the oven at 60 ºC after performing the fracture test. The results obtained (Figure A.6) show a considerably high healing efficiency of 80 %. Nevertheless, it is remarkable how, in contrast with previous results where samples tend to heal strength rather than ductility, for this case the sample becomes much ductile. The increased ductility of the sample can also be attributed to the fact that after keeping the sample in the oven, micro-porosity appeared, as observed in Figure A.7. These results are not conclusive and further testing would be needed.

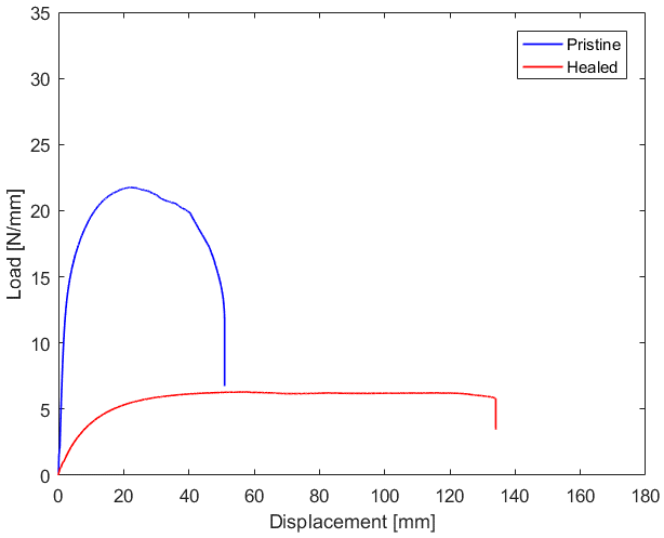

Figure A.6: Fracture tests of M80/H20 for pristine sample and sample healed 1 day at 60 ºC.

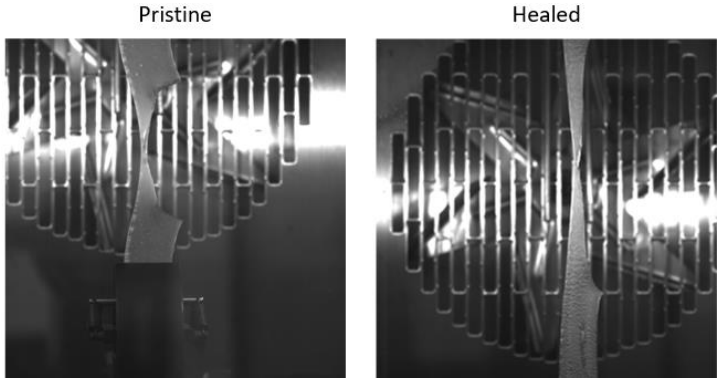

Figure A.7: Optical photos taken for the fracture tests of M80/H20 with healing conditions of 60 ºC and 1 day.